Appl Phys A (2013) 110:281–307
DOI 10.1007/s00339-012-7402-8

Applied Physics A
Materials Science & Processing

INVITED PAPER

Flexible and stretchable electrodes for dielectric elastomer actuators

Samuel Rosset · Herbert R. Shea

Received: 23 September 2012 / Accepted: 24 October 2012 / Published online: 7 November 2012

Abstract Dielectric elastomer actuators (DEAs) are flexible lightweight actuators that can generate strains of over 100 %. They are used in applications ranging from haptic feedback (mm-sized devices), to cm-scale soft robots, to meter-long blimps. DEAs consist of an electrode-elastomer-electrode stack, placed on a frame. Applying a voltage between the electrodes electrostatically compresses the elastomer, which deforms in-plane or out-of plane depending on design. Since the electrodes are bonded to the elastomer, they must reliably sustain repeated very large deformations while remaining conductive, and without significantly adding to the stiffness of the soft elastomer. The electrodes are required for electrostatic actuation, but also enable resistive and capacitive sensing of the strain, leading to self-sensing actuators. This review compares the different technologies used to make compliant electrodes for DEAs in terms of: impact on DEA device performance (speed, efficiency, maximum strain), manufacturability, miniaturization, the integration of self-sensing and self-switching, and compatibility with low-voltage operation. While graphite and carbon black have been the most widely used technique in research environments, alternative methods are emerging which combine compliance, conduction at over 100 % strain with better conductivity and/or ease of patternability, including microfabrication-based approaches for compliant metal thin-films, metal-polymer nano-composites, nanoparticle implantation, and reel-to-reel production of µm-scale patterned thin films on elastomers. Such electrodes are key to miniaturization, low-voltage operation, and widespread commercialization of DEAs.

S. Rosset (✉) · H.R. Shea
Ecole Polytechnique Fédérale de Lausanne (EPFL),
Jaquet-Droz 1, 2002 Neuchâtel, Switzerland
e-mail: samuel.rosset@a3.epfl.ch

Keywords Dielectric elastomer actuators · Compliant electrodes · Carbon · Metal thin-films

1 Introduction

Dielectric Elastomer Actuators (DEAs), also known as artificial muscles, are a new type of soft transducer consisting of a thin elastomer membrane sandwiched between two compliant electrodes. When a voltage is applied between the electrodes, the opposite charges on each electrode give rise to an electrostatic force (Maxwell stress) which squeezes the dielectric layer and causes deformation of the device. The thickness strain s_z caused by the Maxwell stress is defined by [1]:

$$s_z = -\frac{\epsilon_r \epsilon_0 V^2}{Y z^2}, \tag{1}$$

where ϵ_r and ϵ_0 are, respectively, the relative and vacuum permittivity, Y is the Young modulus of the elastomer, and z the thickness of the membrane. Driving voltages are in the order of a few kilovolts, for an elastomer membrane thickness of around 50 µm and with a Young modulus of about 1 MPa, leading to typical compression strains in the range of 10 %–30 % or higher.

The first report of electric field-induced deformation of a solid material is attributed to Alessandro Volta who observed rupture of highly charged Leyden jar capacitors in 1776 [2]. One century later, charge-induced deformation on elastomers was reported by Röntgen [3], and in 2000, Pelrine et al. presented electrostatically activated elastomeric actuators exhibiting surface strains up to 215 % in a landmark publication [4]. This article has marked the dawn of dielectric elastomer actuators, which quickly attracted worldwide attention.

Twelve years after its birth, the field of DEAs has made a giant leap forward, and applications are emerging in many fields and at different size scale, from ocean-wave energy harvesters to haptic feedback devices integrated in smartphones or miniaturized devices capable of mechanically stretching single biological cells [2]. The large strains and intrinsic softness of these elastomeric actuators allow for completely different motion and systems compared to traditional rigid actuators, thus allowing different approaches, such as bioinspired systems [5].

Much research effort has been invested in the selection and optimization of the elastomers used as dielectric [1, 4, 6–10], as well as on applications of DEAs [11]. However, much less attention has been devoted to the devices' compliant electrodes, which are most of the time completely neglected. The fundamental deformation equation (Eq. (1)), which can be found in most of the DEA-related articles, does not take the influence of the electrodes into account and consequently assumes them to be infinitely thin and compliant, which they most certainly are not.

In order to enable the widespread use of DEAs, a number of challenges have yet to be solved: operation at low voltage, miniaturization, large-scale manufacturability and integrated sensing to add "smartness" to the devices. The answer to these key challenges resides in better dielectric elastomer membranes, and also—though often overlooked—in optimized compliant electrodes. This review presents the most important technologies used to make electrodes for DEAs, and explores some new developments for electrode fabrication and application that will open a broad new spectrum of applications, from high-volume production for commercial products, to miniaturized devices with micrometer-sized patterned electrodes.

Strictly speaking, electrodes are not absolutely necessary to induce deformation of a DEA, as shown by Keplinger et al. in a re-enactment of Röntgen's experiment with today's materials [3]. Electric charges can be directly sprayed on the elastomer's surface by an external emitter, causing electrostatic charging and deformation of the soft dielectric due to Maxwell stress. The absence of electrodes presents some undeniable advantages: it avoids the complication of manufacturing compliant electrodes, and the operation in charge-controlled mode (as opposed to voltage-controlled in the case of the standard DEA structure) avoids the electrostatic pull-in instability. Additionally, the deformation is not limited by the stiffening effect of the electrodes, or by the strain at which they lose their conductivity or break. However, if spraying charges on a dielectric is relatively easy, efficiently removing them is more difficult. Electrodes thus allow to bring and remove charges quickly on the elastomer's surface provided they are conductive enough. By patterning the electrodes with precise shapes, they can also bring the charges to precise locations, thus allowing complex structures with several electrically and well defined independent active zones on a single membrane, which is impossible in an electrode-free configuration. These two requirements are very well illustrated by the DEA-based rotary motor from Anderson et al. which combine the need for four separate electrodes on a single membrane with the necessity of high frequency actuation [12]. Electrodes of DEAs are a therefore a practical necessity, and care must be taken in their design in order to profit from their ability to efficiently move the charges at precise locations, without too much impact on the stiffness of the actuator.

2 Stretchable electrodes for soft machines and conformable electronics

Although located on the actuator's surface, the electrodes of dielectric elastomer actuators are at the core of the device's performance: they must be conductive, yet they must be soft; they must sustain large deformations while remaining conductive, yet they must be able to do so for millions of cycles. The life of a compliant electrode for DEAs is a tough one, and it comes as no surprise that the ideal electrode has yet to be developed. However, much progress has been made from the first reported devices whose electrodes were hand-painted carbon grease, and over the years, creative new methods and technologies have started to emerge.

Compliant electrodes are needed in a wide range of applications, well beyond DEAs. Indeed, the booming field of soft and deformable electronics also relies on flexible interconnects that can sustain stretching and/or bending, as recently highlighted in the march 2012 special issue of the MRS Bulletin [13]. The requirements regarding strain amplitude, lifetime and conductivity is quite different between DEAs and stretchable electronics: the electrodes of a DEA must typically sustain biaxial strains of 10 %–100 %, while the deformation of soft electronic circuits is often limited to about 20 % uniaxial or bending strain. An electrode which is highly stretchable will also be bendable, while a bendable electrode is not necessarily highly deformable. DEA must typically survive a large number of stretching cycles (>50 millions cycles in the case of an ocean-wave energy harvester (cf. Sect. 6.4)), while in the case of stretchable electronics it is generally lower and varies from a single deformation in the case of an implantable sensor to several thousand cycles in the case of a wearable flexible displays. Regarding electrical conductivity, flexible electronics require electrodes with a good conductivity to avoid voltage drop along the conductive tracks, while DEAs, being electrostatic devices can tolerate electrodes with a much higher surface resistance, although a good conductivity is needed for high speed operation. Despite these differences, electrodes for DEAs and stretchable electronics have many common characteristics, such as materials, deposition methods and patterning solutions. Consequently, the applications

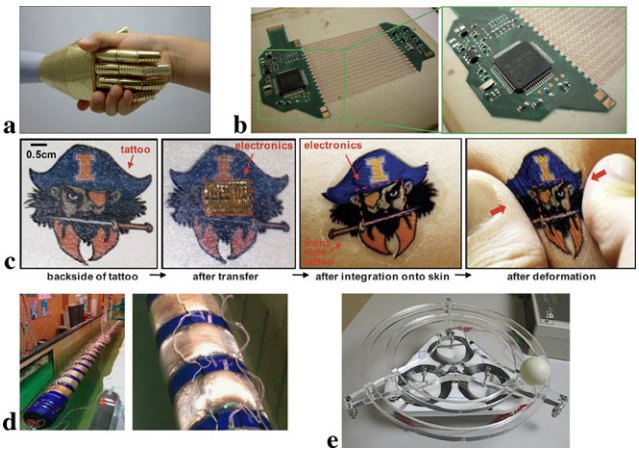

Fig. 1 Application of deformable electrodes: (**a**) Electronic artificial skin with integrated organic transistors and pressure sensors. From [15], ©2012 Materials Research Society. Reproduced with permission. (**b**) Stretchable and deformable interconnects between two PCBs. From [16], ©2012 Materials Research Society. Reproduced with permission. (**c**) Deformable electronic circuit applied on the backside of a temporary tattoo. The circuit and tattoo can conform to the skin and sustain deformation. From [17], ©2011 AAAS. Reproduced with permission from AAAS. d) Dielectric elastomer-based wave energy converter from the company SBM offshore. From [18], ©2012 SPIE. Reproduced with permission. (**e**) DEA-based ring oscillator with smart self-sensing and self-switching integrated on the compliant electrodes. From [19]

of the soft electrodes technologies presented in this review largely exceed the sole domain of DEAs, but encompasses bioinspired stretchable electronics [14], soft electronic skins [15] or PCB-inspired stretchable circuits [16] to give a few examples (Fig. 1).

The electrodes of a DEA are subject to the same amount of deformation as the polymer and must consequently sustain strains typically between 10 %–100 % without being damaged and while remaining conductive. Their mechanical impact on the stiffness of the dielectric must be low to avoid reducing the strain output. In one word, they must be *compliant*. As stated by Pelrine et al.: "The ideal electrode would be highly conductive, perfectly compliant and patternable, and could be made thin relative to the polymer thickness" [1]. The general compromise found in the first EAP-related publications is to use electrodes based on carbon powders applied with a brush or a spray, which—except for the compliance—are far from the perfect electrodes described by Pelrine. Graphite and carbon black powders, conductive carbon grease, or carbon powders in an elastomeric matrix were the first types of electrode used, because of their low stiffness and ability to remain conductive at large strains [1, 4, 20, 21]. Although well-adapted to lab experimentations, carbon-based compliant electrodes applied with a paintbrush have limitations in terms of patternability, scalability for large-volume production, compatibility with clean-room processes, reliability, lifetime and ease of application. To overcome these limitations, new types of electrode have emerged over the last few years. Metallic thin films, although not intrinsically stretchable beyond a few percent, can be patterned in-plane or made to ripple out-of-plane, and can then remain conductive and undamaged at strains above 30 %. Other methods including nano-composites are also emerging, based on metal ion implantation, platinum salts, exfoliated graphite or carbon nanotubes.

In the following sections, the different compliant electrodes used for DEAs will be presented, starting with the most widely used carbon-based electrodes (Sect. 3), followed by the metal thin-film electrodes (Sect. 4), and finally by some emerging more exotic methods (Sect. 5). The main characteristics of each electrode type are investigated, as well as the methods available to pattern these electrodes on thin elastomeric substrates. In the discussion (Sect. 6), several practical applications (miniaturization, reduction of driving voltage, integrating sensing and energy harvesting) are presented; the impact of the electrodes for each of these examples is examined in detail.

3 Carbon-based electrodes

3.1 Carbon powder, grease, and rubber electrodes

The most commonly used electrodes for DEAs are based on carbon particles and can be categorized in three main variants (Fig. 2): loose particles of carbon simply deposited on the elastomeric membrane; carbon grease, which consists of carbon particles dispersed into a viscous media such as oil; and conductive rubber, which is formed by dispersing carbon particles into an elastomer, which is crosslinked after it has been applied on the membrane.

Carbon powder One of the main advantages of powder-based electrodes is that they do not contribute to the stiffness of the membrane on which they are applied, due to the absence of a strong binding force between the agglomerates. Loose carbon powders (mainly carbon black and graphite), directly applied on the dielectric membrane, were thus the material of choice in the early days of DEAs, as they allow demonstrating the large strain capabilities of these soft actuators. Although metals are intrinsically more conductive than carbon, their powders have a tendency to form an insulating oxide layer at the surface [23]. Additionally metal particles are too large to create sufficient contacts, and a better conductivity can be obtained with carbon particles [24]. Metallic powders are therefore rarely used for DEAs, although a few articles report on the use of silver grease electrodes [25, 26]. The relatively high electrical resistance of carbon-based electrodes does not play a primary role for

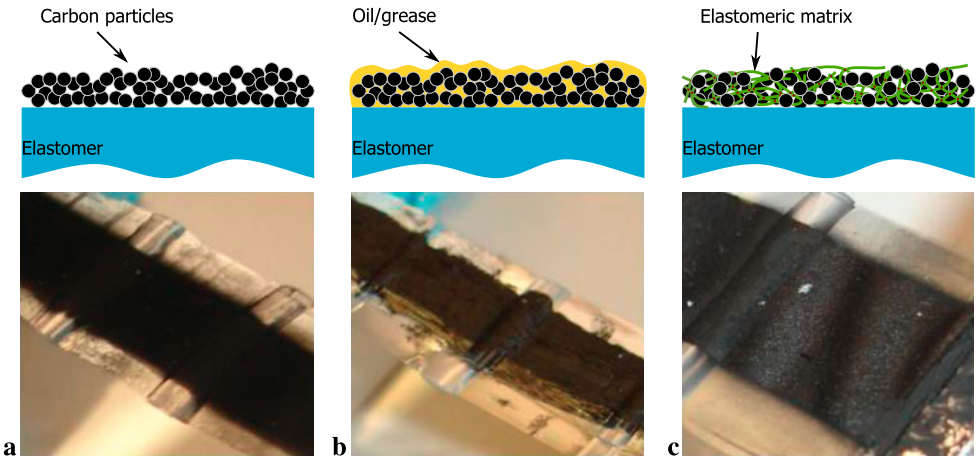

Fig. 2 The three main types of carbon-based electrode. (**a**) Loose carbon powders consists of carbon black (or graphite) particles directly applied on the elastomer membrane. (**b**) Carbon grease consists of carbon particles dispersed in a viscous oil. (**c**) Conductive rubber consists of carbon particles dispersed into a crosslinked elastomer. Photos adapted from [22], ©2007 SPIE. Reproduced with permission

actuators, as long as the electrical time constant of the device remains smaller than the mechanical bandwidth. For instance a 1 cm^2, 40 µm thick DEA with a silicone membrane has a capacitance of about 65 pF. With electrodes whose resistance would be in the M Ω range, it could still be driven up to 1 kHz.

In addition to being quite difficult to handle due to their high sensitivity to static charges, loose powders present several disadvantages: maintaining full coverage at large strains is difficult, [9, 27] and the lifetime of the electrode is limited due to the possibility of the conductive particles to detach from the electrode. Consequently, electrodes with loose powders are mainly found in combination with adhesive acrylic elastomers (such as VHB from 3M) as dielectric layer: because this material is intrinsically sticky, the conductive particles become bound to its surface. A notable exception where loose graphite powder electrodes are used in combination with a silicone elastomer is in the multilayer process of Prof. Schlaak's group [28–31]. But as each electrode is effectively covered by the next dielectric layer, one cannot strictly speak of loose powders for this particular case.

Carbon grease One way to solve the issues mentioned above is to bind the powders into a viscous matrix, such as grease. Although easier to handle than loose powders and capable of sustaining larger strains while remaining conductive, carbon-grease electrodes also have disadvantages: grease can have long term stability issues caused by drying or diffusion into the dielectric membrane, which can cause short circuits or swelling of the elastomer membrane. As any viscous material, grease also creeps under gravity, which negatively impacts the lifetime of these electrodes, particularly for devices stored vertically. The absence of a reliability study on these kinds of electrode (and DEAs in general) makes it difficult to assess the importance of these factors. Furthermore, grease, similarly to loose powder, can be subject to mechanical abrasion, which also negatively impacts the lifetime.

Conductive rubber Finally, the conductive carbon black particles can be incorporated into an elastomer matrix, such as a silicone, which is cured after the electrode is applied on the membrane, in order to obtain a polymer-carbon conductive composite. Because in that case the electrode is bound to the membrane, it is much less prone to ablation or migration of the electrode material with time, which positively impacts the electrode's life expectancy. However, because of the elastomeric matrix, the electrode's contribution to the stiffness of the elastomer cannot be neglected anymore, compared to carbon powder or grease. As Pelrine et al. pointed out, these types of electrode work best for thicker dielectric films, i.e. when the thickness of the electrode is negligible in comparison with the thickness of the dielectric elastomer [1]. The stiffness of an elastomer-carbon black compound is very dependent on the quantity of filler particles, which must be sufficiently high to be above the percolation threshold. The percolation threshold is very dependent on the surface area of the carbon black, as well as the matrix in which it is dispersed and can vary between 1 %–24 % [23]. In silicone, we have observed a percolation threshold of about 6 % for Ketjenblack EC-300J from AkzoNobel, and of about 3 % for Ketjenblack EC-600JD, due to its extremely high surface area (1400 m^2/g according to the datasheet, compared to 800 m^2/g for the former)[1]. With graphite (4206 from Merck) in DowCorning Sylgard 184, Kofod observed a percolation threshold of 23 % [32].

Assuming the same silicone is used to produce the dielectric membrane and the conductive electrodes, the mechanical stiffness of the filled polymer will be larger than the membrane's, thus showing the importance to apply the material in a very thin layer.

The main carbon-based compounds reported in literature for the fabrication of compliant electrodes for DEAs are summarized in Tables 1, 2 and 3. In addition to these three

[1] Unpublished results.

main types of carbon electrode for DEAs, some other ideas have been presented, for example using carbon nanotubes (cf. Sect. 5.3) or exfoliated graphite [39].

Table 1 Main carbon powder-based compounds used to make electrodes for DEAs

Type	Name	Ref.
Carbon black	Vulcan XC72	[32, 33]
Carbon black	Ketjenblack EC-300J	[32, 34, 35]
Carbon black	Ketjenblack EC-600JD	[36]
Graphite	N-77 (Spray)	[20]
Graphite	Merck 4206	[32]

Table 2 Main carbon grease-based compounds used to make electrodes for DEAs. * indicates a compound prepared in the research laboratory

Name	Ref.
CW 7200, *Chemtronics*	[9, 20]
Nyogel 755G, *Nye Lubricants*	[37]
Nyogel 756G, *Nye Lubricants*	[19]
PDMS oil + Ketjenblack EC-300J*	[32]

Table 3 Main conductive rubber-based compounds used to make electrodes for DEAs. * indicates a compound prepared in the research laboratory

Composition	Ref.
RTV 60-CON, *Stockwell*	[9, 25]
Rhodorsil CAF4, *Bluestar* + Vulcan XC72*	[33]
RTV23, *Altropol* + KB EC-300J*	[35]
Elastosil E43, *Wacker* + KB EC-300J*	[32]
Sylgard 184, *DowCorning* + Vulcan XC72*	[38]

3.2 Application methods for carbon electrodes

While simple prototypes and demonstrators can be manufactured without much regard of the shape, precision and thickness homogeneity of the electrodes, which can simply be *smeared* on the elastomeric membrane [19, 21, 37, 40], most actuators for commercial applications require electrodes of a precise shape, patterned on a cm, mm, or even µm scale. Several techniques can be used to apply and pattern carbon electrodes on a dielectric elastomer (Fig. 3), as described in the next paragraphs.

Shadow masking A shadow mask, or stencil can be placed on the elastomer membrane to selectively expose the surface that needs to be coated with the conductive material [1]. If the thickness homogeneity and reproducibility is not a main concern, the conductive solution can be simply applied on the mask with a brush, which has been demonstrated by Pelrine et al. for loose powders and carbon grease [9]. For better uniformity, spray coating can be used in combination with a shadow mask to apply a thin uniform layer on the elastomeric membrane. For their automatized stack process, Schlaak et al. have tested spray coating through a shadow mask of both dry graphite powder and graphite in suspension in isopropanol [28–31, 41]. With their process, which alternates between the application of a silicone layer by spin coating, the heat-activated cross-linking of the silicone, and the subsequent deposition of the electrodes (Fig. 4), they have developed an efficient production method, which allows building actuators of up to 100 layers with a production time of 5 minutes per layer, thus demonstrating that carbon electrodes can also be used for larger scale and commercial applications. Araromi et al. reported on a similar stacked actuator fabrication process with a sequence of silicone and electrode deposition by spray coating with an airbrush [42]. Because the dielectric layer is also sprayed, there is no need for a spin-coater, thus reducing the cost of the installation.

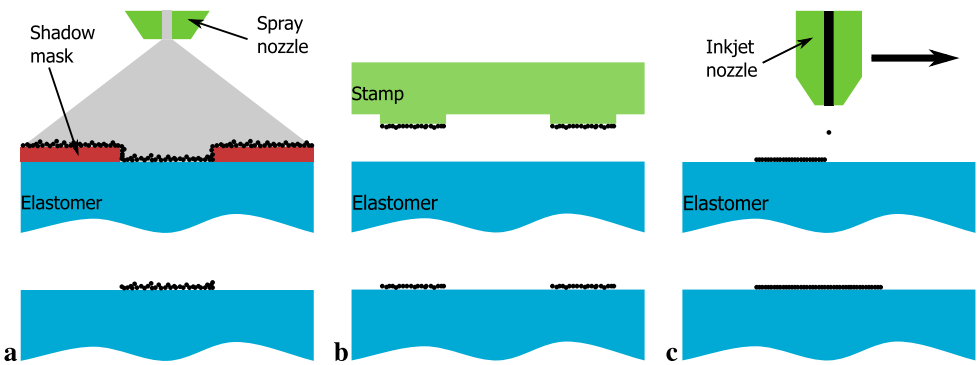

Fig. 3 Different ways to pattern carbon electrodes. (**a**) Using a shadow mask to selectively protect part of the elastomeric membrane. The carbon-based electrode material can then be dispensed (for example by spraying) on the surface. The shadow mask is subsequently removed to expose the patterned electrode. (**b**) Using a patterned elastomeric stamp to pick-up the electrode material and apply it on the elastomeric membrane. (**c**) Using standard printing techniques, such as drop-on-demand inkjet printing

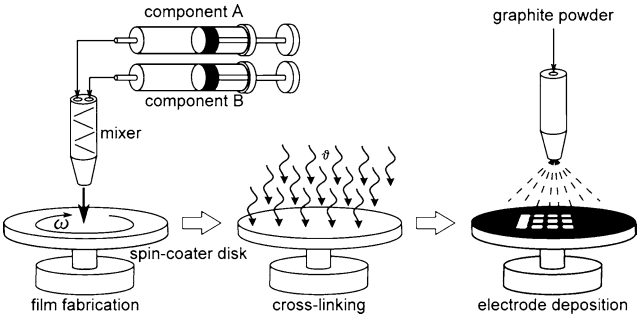

Fig. 4 Main process steps of the Schlaak et al. process for manufacturing stacked DEAs with patterned carbon sprayed electrodes. From [31], ©2011 IEEE. Reproduced with permission

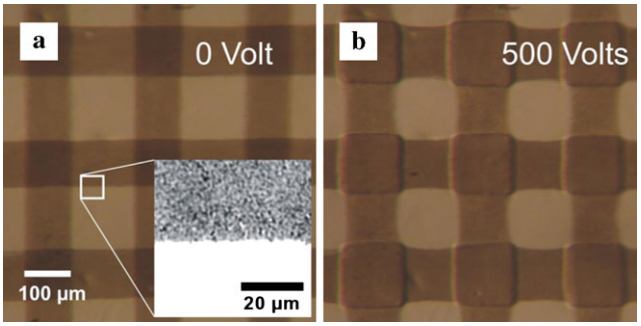

Fig. 5 100 µm-wide loose carbon black electrodes applied with a structured stamp on an acrylic elastomer membrane. From [43], ©2007 SPIE. Reproduced with permission

Their electrode consists of graphite powder put in suspension in a solvent (1:4 ratio). Spray coating through a shadow mask can also be used with conductive rubber if mixed with solvent to decrease viscosity [32, 35].

One drawback of using a stencil to define the shape of the electrodes is the contact between the mask and the elastomer membrane, particularly in the case of very thin suspended membranes. If applying the mask and spraying the electrode can be done quickly, removing the mask at the end of the process must be done slowly and carefully in order not to damage the membrane stuck on the mask. Leaving a small gap between the mask and the membrane is not advisable because shadowing will occur at the mask border and the airflow from the spray coating system can deform the membrane, leading to a loss of resolution.

Stamping Patterned structures can also be obtained by stamping the conductive electrode on the dielectric membrane. A soft stamp with the desired pattern is fabricated, for example by replication on an etched silicon negative master. Small structures and a good resolution can be obtained with this method. For instance, Aschwanden and Stemmer have used this technique to pattern 100 µm-wide lines with loose carbon black powder on an acrylic elastomer (VHB 9460) membrane [43]. The lines of electrodes on both sides of the membrane formed a matrix of 100 µm × 100 µm actuators which exhibited up to 35 % linear strain for a 500 V actuation voltage (Fig. 5). Stamping loose carbon black powder is made possible for this particular application by the use of the VHB adhesive as dielectric layer: the stickiness of the surface ensures the transfer of the carbon particles from the stamp to the membrane, and fixes them on the elastomer surface. Commercially available stamping techniques can also be used with carbon grease or conductive rubber when adequately diluted to form a *conductive ink*.

Printing techniques There is still room for development of effective, rapid and high-resolution patterning techniques for carbon-based electrodes for DEAs. The three major types of carbon electrode presented here can be prepared in the form of a conductive ink, and most of the techniques developed for the printing industry, including inkjet printing, screen printing or roll-to-roll processes, can be applied to pattern conductive electrodes on elastomers. The polymer solar cell community, for example, is using these printing methods for the manufacturing of flexible devices [44]. Their production lines require high throughput, the coating of large surfaces, and the patterning of precise features (down to the µm scale). This is similar to the needs of compliant electrodes for DEAs in case of a large-scale commercial application.

Among the standard printing methods, inkjet printing is particularly interesting, because it is a purely non-contact method, and it is therefore well-adapted for thin suspended membranes. This is a versatile method, as the shape of the electrode can be adapted at will just by modifying the bitmap used to print the electrode. This represents a very interesting advantage over shadow masks for the research community, because different designs can quickly be printed and tested, which allows for quick optimization of the electrode shape. Large-scale printers with multi-nozzle (up to 1000) printheads are capable of large throughput, which renders this technique also attractive for commercial high-volume production of DEAs. A major difficulty resides in the development of a jettable ink for EAP applications, which is not a straightforward task. The parameter space is limited by a large number of factors: first, there are the printer/nozzle requirements on liquid viscosity, surface tension and vapor pressure, which must be followed in order to obtain regular and stable generation of drops on demand. These requirements are nozzle-related and can be quite tight. For example, the R&D printer Dimatix DMP-2800 from Fujifilm requires inks with viscosities between 10 and 12 mPa s, and surface tension between 22 and 33 mN/m. To avoid clogging the small nozzle orifices (typically 10–100 µm depending on manufacturer), the carbon particles must be carefully dispersed and no flocculation or sedimentation is allowed. The evaporation rate of the ink must not be too high, to avoid

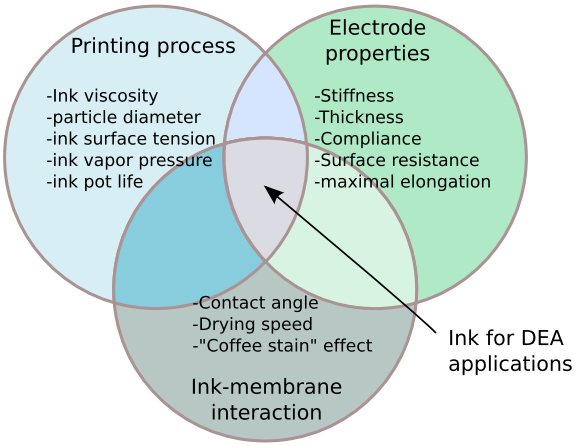

Fig. 6 Schematic representation of the reduced parameter space available to design an inkjettable ink for DEAs application. The fluid must fulfill the requirement of the printer's manufacturer in order to be reliably dispensed. Once the ink droplets reaches the polymer's surface, it must cover it and dry uniformly, and finally the cured ink must be conductive and compliant in order to be used for DEAs

clogging the nozzle when it is not jetting (i.e. when the nozzle is traveling above a zone which must remain free from ink). Secondly, the interaction between the droplet and the membrane, once the former reaches the latter, adds further requirements on the fluid formulation. The contact angle between the ink and the elastomer must be low enough to obtain good wetting. If the contact angle is too high, there is a risk that adjacent droplets merge together and form a large ink pool, causing a dramatic loss of resolution. This is especially problematic with silicones, which have a very low surface energy and present highly hydrophobic surfaces. Different surface treatments (plasma activation, UV exposure) can help to temporarily increase the surface energy, and Robinson et al. have recently demonstrated how the wetting of a silicone substrate by a solvent-based ink can be improved by structuring the silicone substrate with micropillars [45]. The ink's evaporation rate must be controlled so as to avoid the "coffee stain" effect, which is caused by the motion of the ink's solid content to the periphery of the droplet, leading to a non-uniform coating once the layer is dry. This effect can be avoided by carefully choosing the solvents used for the ink formulation, using a mix of solvents with different vapor pressures [46]. Finally, the ink formulation must be selected so that the dry and cured film fulfils the requirement for compliant electrodes: low stiffness, compliance, conductivity etc. Figure 6 illustrates the requirement that an ink formulation must fulfil.

3.3 Electrical properties of carbon electrodes

Because of the absence of suitable commercial products, most carbon-based compounds are prepared in research laboratories, with different amount of fillers, different degrees of dispersion of the agglomerates, and applied in a broad range of thicknesses. Consequently, a large spectrum of surface resistance has been reported in the literature. Kornbluh et al. commented on this large resistivity spectrum by stating: "Typical surface resistivities of our electrodes are on the order of tens to hundreds to thousands of ohm" [8]. Toth and Goldenberg measured a surface resistance of about 20 k$\Omega/\square$ for carbon grease. They observed an exponential increase of the electrodes resistance when submitted to an uniaxial strain, which they modeled with the following equation [25]:

$$R = R_0 \beta^{(\alpha-1)}, \tag{2}$$

where R is the resistance of the stretched electrode, R_0 the initial resistance of the undeformed electrode, α the uniaxial stretch, and β a constant characterizing the sensitivity of the resistance to strain. They tested different types of electrode and reported the following values for β: 4 for carbon conducting grease, 6.5 for conducting RTV silicone, 6.8 for silver conducting grease, and 22 for graphite powder. Carbon-grease electrodes was thus expected to remain conductive at larger strain compared to the other electrodes tested in the study. Carbon grease is thus the electrode material used by Keplinger et al. to demonstrate gigantic strain (1692 % surface strain) on a DEA balloon, using instability snap-through [47]. However, with another home-made carbon grease, Kofod observed that grease migration starts to occur at large strains (above 100 % biaxial), and full coverage of the electrode surface is not ensured anymore [32]. This highlights how the electrical properties (initial resistivity and behavior when strained) of home-made carbon-based compounds depend on the method of preparation.

In addition to their primary role of transporting and storing the charges for the generation of the electrostatic force (and hence actuation), the electrodes, and their change in resistance while being deformed can be used to monitor the strain and operate the actuator in closed-loop mode. O'Brien et al. characterized the three main types of carbon-based electrode (loose powder, grease and conductive rubber) for resistive self-sensing (Fig. 2) [22]. For the three electrode types, they obtained a surface resistance of about 9 k$\Omega/\square$. The electrodes were then submitted to uniaxial strain, while measuring the change in resistance for self-sensing applications. Loose carbon powder exhibited the best resistance as function of strain behavior: no noise, and no overshoot, while carbon grease produced a noisy signal and bound carbon powder—although mechanically the best—presented a time-dependent signal with strong overshoot at each change in strain rate (Fig. 7). As explained by Wang et al., the resistance time-dependency of a carbon-filled elastomer exhibit the same forms as the corresponding mechanical properties of a viscoelastic material, thus explaining the jumps in resistance at the times at which the strain rate is modified [48].

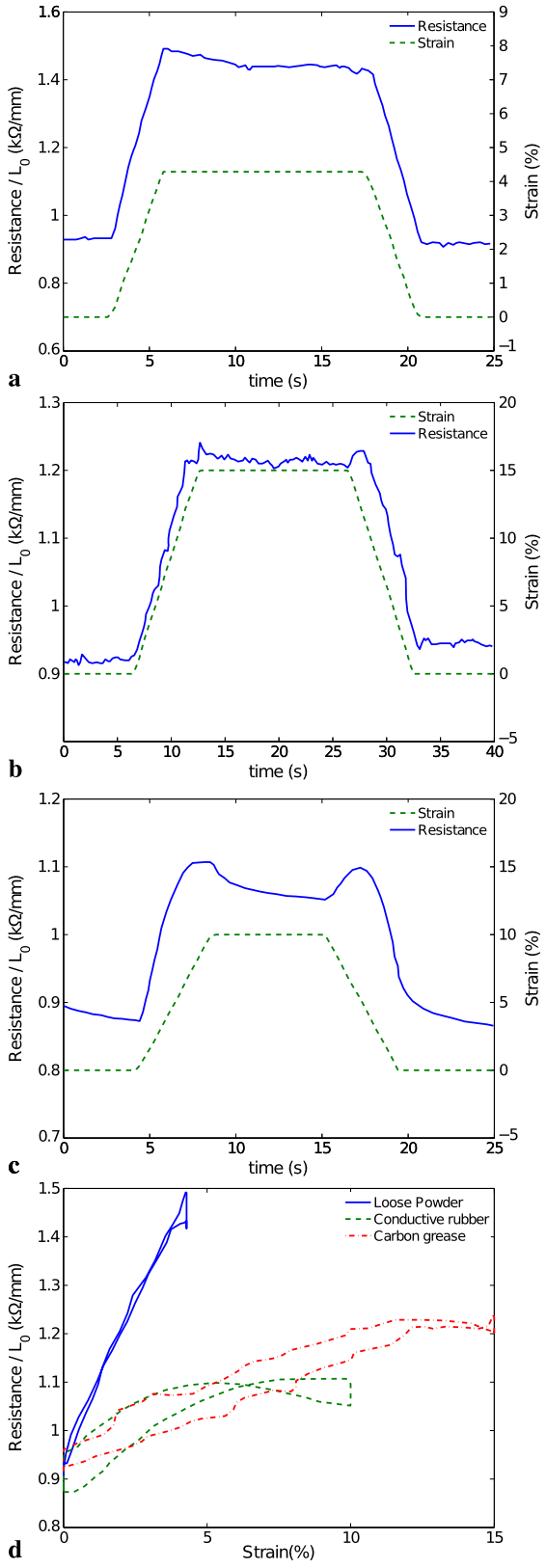

Fig. 7 Change in resistance (normalized to the initial track length) of carbon-based compliant electrodes submitted to uniaxial stretching. (**a**) Loose carbon powder, (**b**) conductive rubber and (**c**) carbon grease. (**d**) Normalized resistance as a function of strain for the three types of electrode. Adapted from [22]

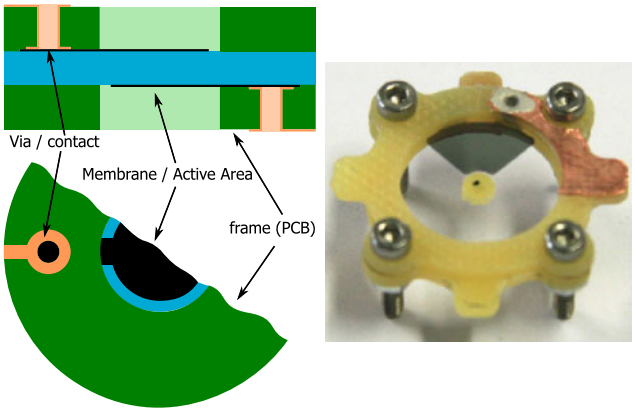

Fig. 8 *Left*: example of interface between a compliant electrode and an electronic circuit with the help of a double-sided PCB playing the double role of a support frame and electrical interface through the use of metallized vias. *Right*: application of the concept to a DEA with a home-made single-sided PCB. The absence of copper on the backside (in contact with the electrode) is compensated with a conductive silver varnish in the via hole

The plot of the resistance as a function of the applied strain shows the lack of hysteresis of the loose carbon electrodes compared to the two other alternative, which is very important for self-sensing applications (Fig. 7(d)). One also notes the higher sensitivity of the resistance of loose carbon powder electrode compared to grease, which is in good agreement with the empirical relation and observations of Toth and Goldenberg reported in the previous paragraph.

Compliant electrodes are necessary to obtain a large displacement of the active area (the zone which is covered by two electrodes). In order to bring the electrical charges that will create the electrostatic force and the displacement of the active zone, it is necessary to connect one end of the electrode to a high-voltage power supply. The interface between the electronic driving circuit and the soft electrodes must be made in a way to ensure a reliable electrical contact without damaging the electrodes and while assuring a long lifetime of the interconnect. Because of their crosslinked state and good adhesion to the dielectric elastomer layer on which they are applied, conductive rubber electrodes are easier to reliably connect to an external rigid electrical connection point compared to loose powder or carbon grease. There are several methods to connect an electrode to the driving circuit. One possibility in the case of suspended membranes is to combine the supporting frame holding the membrane with the electrical contact interface, by using an insulating structure with conductive tracks, such as a printed circuit board (PCB). It is then possible to integrate the actuator with the electrical driving circuit on the same board (Fig. 8).

4 Metallic thin-film electrodes

The microelectronics and MEMS industry has developed a broad range of microfabrication technologies to create pat-

terned conductive thin films. Metals can be deposited in thin layers on a broad range of substrates by electron beam evaporation, cathodic sputtering, or electroplating and patterned down to the nm scale using photolithographic processes. Reproducible results at a large throughput can be obtained with these methods (for instance over one billion interconnects on modern microprocessors), which consequently have the potential of moving the EAP technology from the lab to the industry. The ability to pattern the electrodes on a small scale allows for the fabrication of many electrically independent actuators on the same membrane, which paves the way for a broad range of new applications based on arrays of microactuators.

However, there are two major obstacles to the direct use of metal thin film as electrodes for DEAs. First, the Young modulus of metal is several order of magnitude higher than that of dielectric elastomers (50–100 GPa compared to 0.2–1 MPa), which means that even 50 nm-thick electrodes on a 50 µm-thick elastomer will have a significant stiffening impact on the elastomer, leading to a negligible actuation strain. For example, we have shown that sputtering a 8 nm gold layer on a 30.6 µm PDMS membrane with an initial Young's modulus of 0.77 MPa caused a relative increase of the Young modulus of the membrane of 440 %, up to 4.2 MPa [49]. Secondly, the limit of elasticity for metals is very low, typically 2–3 % and if a metal electrode is strained above this limit, it will crack and form islands separated by non-conductive polymer.

Despite this limitation some research groups proposed and tested clever solutions to use metallic thin films for DEA applications, even though they present a very high Young's modulus and a low limit of elasticity. These methods, summarized in Fig. 9, include the use of patterned electrodes (Sect. 4.1), of out-of-plane buckled electrodes (Sect. 4.2), and of corrugated membranes (Sect. 4.3).

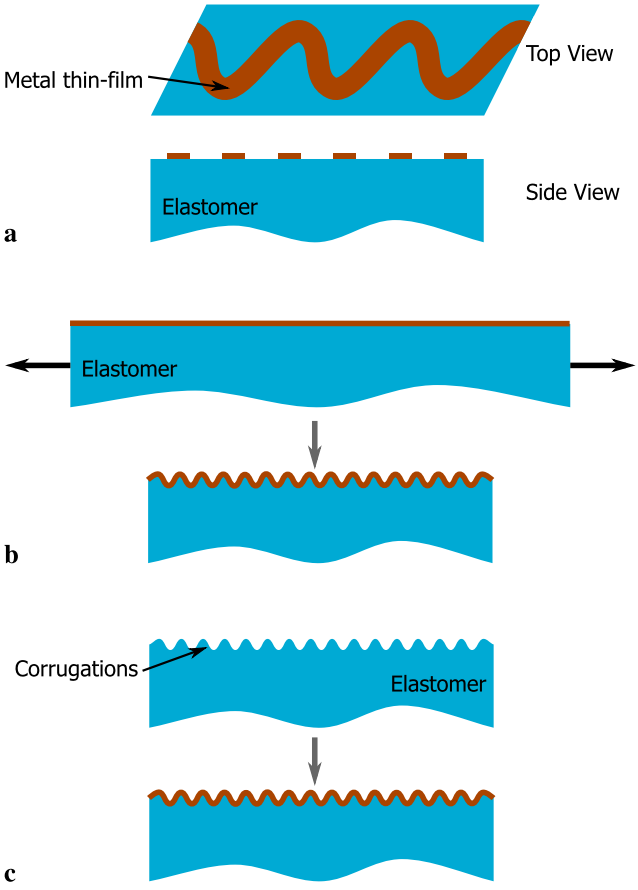

Fig. 9 Different methods to create stretchable electrodes based on metal thin films. (**a**) Using a patterned electrode defined by photolithography instead of a plain electrode. (**b**) Depositing the metallic thin film on a stretched elastomeric membrane, in order to create out-of-plane buckling when the substrate is relaxed. (**c**) Fabricating a corrugated elastomeric membrane on which to deposit the thin-film electrode

4.1 Patterned metal electrodes

Patterning metal traces can be used to define several independent devices on the same membrane, but on a smaller scale, it can also be advantageously used to replace a sheet (i.e. continuous) electrode by a patterned one (Fig. 10). When carefully designed, the patterned electrode still allows for the membrane to move and expand in the desired direction without damaging the metallic thin film. Compared to a plain electrode with the same external dimension, the patterned electrode has a smaller active area, and therefore the capacitance formed by two aligned electrodes between an elastomeric membrane is lower, leading to a smaller electrostatic force and strain. However, if the patterned structure is carefully designed, the capacitance can be increased due to the fringing field capacitance, and approach that of plain electrodes.

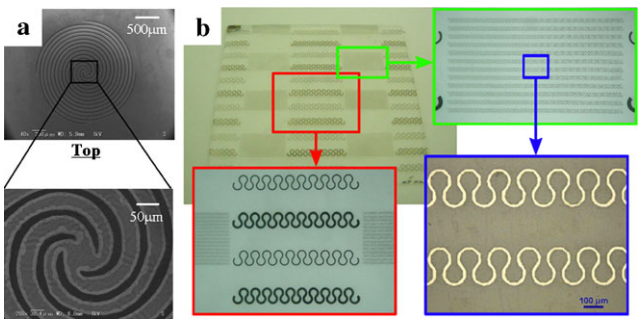

Fig. 10 Patterned compliant metal thin-film electrodes. (**a**) 170 nm Cr/Au/Cr electrodes evaporated on a 30–40 µm-thick DowCorning Sylgard 186 membrane and patterned to optimize out-of-plane displacement of the diaphragm. Adapted from [50], ©2007 IEEE. Reproduced with permission. (**b**) Horseshoe-shaped metal tracks optimized for uniaxial extension. From [51], ©2012 IOP publishing Ltd. Reproduced with permission

Pelrine et al. have deposited a thin layer of gold (<100 nm) on an elastomeric membrane by cathodic sputtering. The layer was subsequently patterned by photolithography to form zig-zags with a conductive width down to 5 μm [9, 27]. They report that the electrodes can be stretched in the direction of the zig-zags up to 80 % while remaining conductive. It should be pointed out that the mechanical properties of a membrane with such zig-zag electrodes patterned on its surface become anisotropic, and that the membrane is softer in the direction of the zig-zags than across them. When used for DEAs these electrodes promote uniaxial strain, which can, depending on the practical application in which the actuator is intended to be used, be seen as an advantage or a disadvantage. To reduce the stiffening impact on the membrane, the zig-zag electrodes of Pelrine et al. are separated by a space many times their width. Consequently, to ensure a better electric field coverage, the authors point out that a second electrode material is necessary to carry the charges in-between the zig-zag traces, and they have shown that the humidity contained in ambient air makes it sufficiently conductive to conduct charges between two gold traces, if speed is not an issue.

Although not directly targeted at DEAs, Gonzalez et al. have studied the maximal elongation of meandering metallic tracks deposited on a silicone elastomer and submitted to uniaxial strain (Fig. 10(right)) [52]. The authors have conducted FEM simulations to optimize the shape of the meanders in order to maximize the elongation of the conductive track at break. They found that a "horseshoe" shaped track with a conductive width as small as possible was the best solution, and they reported elongation at break up to 100 %, which is slightly above the non-optimized zig-zags tracks of Perlrine et al. presented in the previous paragraph. The technique was further developed by Verplancke et al. by sandwiching the meandering track between two spin-coated polyimide layers as a means to improve mechanical performance [51]. They obtained reproducible uniaxial stretching up to 100 % without noticeable change in resistance ($R_0 \approx 180\ \Omega$) or hysteresis. A life time of 500000 stretching cycles has been demonstrated for a strain of 10 %.

Pimpin et al. have designed a diaphragm microactuator capable of out-of-plane buckling made with a 180 nm gold electrode deposited by e-beam evaporation. A 10 nm chromium adhesion layer was deposited first, followed by the gold layer and a final chromium layer to avoid stress gradients. The metallic layer was finally patterned in concentric rings to form a compliant electrode [50, 53]. This example is particularly interesting, because it presents a small-size device (2 mm diameter) made in a clean-room environment with microfabrication production methods. Carbon-based electrodes are consequently out of question for this process, and using electrodes patterned in concentric rings is a clever workaround. To obtain the best strain performance, the electrodes must be carefully designed. For example increasing the spacing between the conductive tracks while keeping the width of these lines constant reduces the stiffening effect of the metal, but reduces the effective area of the electrode. Pimpin et al. have conducted FEM simulations and experimental verifications to optimize the fill factor of their patterned electrode. Taking the width of the conductive tracks w, the gap between the concentric rings g, and the thickness of the dielectric membrane h, they found that the displacement was maximized when the electrodes have a g/w ratio of 0.33, and a w/h ratio as small as possible. Consequently, g should be made as narrow as the patterning process allows, and w three times larger than g. With $g = 7$ μm and $w = 23$ μm, the authors obtained a static deflection of 112 μm at an applied electric field of 75 V/μm, which represents 5.6 % of the membrane's diameter. The authors also tested unpatterned electrodes of the same total size and obtained a static displacement six times smaller, thus showing the necessity of patterning a metallic thin-film electrode when used for DEAs. However, even with the patterned electrode, the 5.6 % height over diameter ratio is not a large strain: assuming the membrane's buckled shape is a spherical cap, this vertical displacement corresponds to a surface strain of the membrane of 0.31 %. On the same elastomer (Dow Corning Sylgard 186) but with extremely compliant electrodes made with carbon grease, we have measured surface strains of 14.8 % at the same applied field.[2]

4.2 Out-of-plane buckled electrodes

The high coefficient of thermal expansion of silicones ($9 \times 10^{-4}\ \mathrm{K}^{-1}$ (volume) for Dow Corning Sylgard 186 according to the datasheet) is often problematic when they are used in conjunction with other materials with much lower thermal expansion. However, this property can be advantageously used to make compliant electrodes out-of-plain metallic thin films. In a letter to Nature, Bowden et al. showed how they were capable of creating complex out-of-plane structures by depositing a thin-metallic film (50 nm) by E-beam evaporation on a piece of heated silicone (Fig. 11) [54]. The contraction of the silicone when it was cooled down to room temperature created a compressive stress in the metallic thin film, causing it to buckle out-of-plane, forming an undulating structure with a wavelength of 20–50 μm. These kind of structures can be induced either by heating the silicone substrate, or just by using the heat generated by the deposition process. Lacour and Wagner evaporated 100 nm-thick gold tracks that were 28 mm long and 0.25 mm wide on a 1 mm-thick silicone substrate and observed the formation of out-of-plane structures perpendicular to the track

[2] Unpublished results.

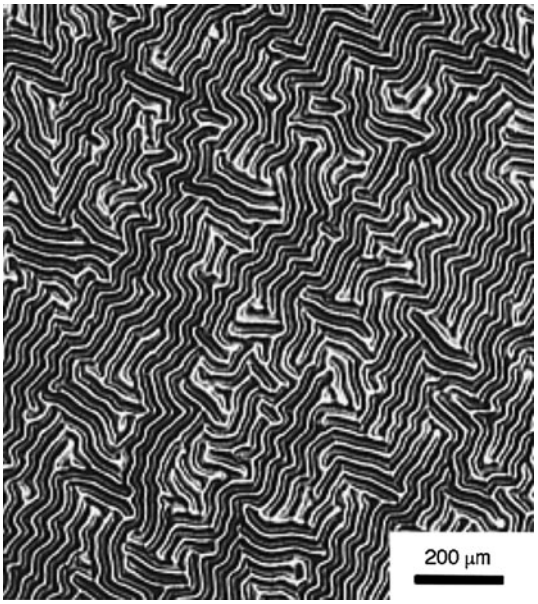

Fig. 11 Out-of-plane buckling of a thin-metallic film deposited on an elastomer membrane due to different coefficient of thermal expansion. From [54], ©1998 Macmillan Publishers Ltd. Reproduced with permission

length [55]. They measured the resistance increase of the track when submitted to uniaxial strain, and observed that it remained conductive for strains up to 23 %, which greatly exceeds the yield strain of gold. This is due to the fact that the out-of-plane waves flatten out when the composite is stretched. Similar out-of-plane wavy electrodes induced by thermal stress have also been reported by Maghribi et al. for a stretchable micro-electrode array [56].

Controlling the amplitude of the out-of-plane structures is difficult if one relies uniquely on the thermal stress induced during the deposition. However, generating compressive stress in the mechanical layer is also possible by prestretching the elastomeric substrate before the deposition of the metallic thin film (Fig. 9(b)) [55, 57]. Lacour et al. have uniaxially prestretched a silicone substrate by 10 %–20 % before depositing a 25 nm-thick gold layer [55]. Following deposition and patterning of the metallic tracks, the substrate was allowed to relax, leading to out-of-plane buckling of the gold electrode. The resistance of 0.5 mm $\times$ 4.6 mm stripes was measured as a function of strain. Electrodes that were evaporated on a substrate that was stretched 15 % during the deposition process could be uniaxially strained up to 28 % before losing conductivity because of crack formation in the metallic layer. It should be pointed out that this value is far superior to the 15 % strain state applied during the electrode deposition, strain at which the out-of-plane waves are expected to completely disappear when subsequently stretched in the same direction. After the release of the 15 % deposition prestretch, the metallic stripes formed a sinusoidal profile with wavelength of 8.4 μm and an amplitude of 1.2 μm. The authors report on a large variation of the initial surface resistance of the stripes, from 0.8 Ω/□ up to several MΩ/□ [55]. The sample whose resistance was characterized as function of strain had an initial surface resistance of ∼14 Ω/□. Upon uniaxial stretching, the resistance of the stripe decreased down to ∼8.2 Ω/□, for a strain of 17 %, i.e. slightly higher that the deposition prestretch. At higher strain, the surface resistance increases slowly. Above 28 % strain it rises sharply up to electrical failure. Cyclic testing of up to 100 cycles have shown that the samples remain stable. To apply this kind of electrode to DEAs, however, the cyclic loading tests should be pushed further. This method can also be used with a biaxial prestretching for deposition, in order to make actuators capable of expanding in the two in-plane directions, depending on the application.

Electrodes which remain conductive when stretched are one of the two important requirements for compliant electrodes for DEAs, the second being a negligible stiffening impact on the dielectric membrane. This effect has not been analysed for these buckled electrodes, and they have not been directly applied to build and characterize DEAs. However, their close similarity with the corrugated electrodes (cf. Sect. 4.3) which have been successfully used to make reliable DEAs, indicates that similar performance should be expected.

4.3 Metal thin-film electrodes on corrugated membranes

One of the main limitations of the method presented in the previous paragraph is the need for mechanically prestretching the membrane. Metal thin-film deposition and patterning via photolithography are methods which are compatible with a microfabrication process flow, but prestretching is not, due to the need to remove the membrane from its substrate, mechanically deform it and fix it on a retaining frame. As an alternative method to mechanical or heat-induced prestretch to generate out-of-plane wavy electrodes, Benslimane et al. have introduced the use of a structured dielectric elastomer membrane [58]. The silicone elastomer is applied on a mold with a quasi-sinusoidal corrugation profile. After curing, the membrane is separated from the mold, and a 70–110 nm thick Ag thin film is deposited on the corrugated side. The wave profile of the mold has been optimized to obtain elongations of 33 % in the compliant direction before the metallic electrode breaks. The capacitor configuration needed for DEA applications is obtained by laminating two films together with their flat sides in contact (Fig. 12). The lifetime of the corrugated electrodes was investigated by cyclic activation of an actuator with corrugated electrodes. The test setup consisted of two membrane actuators mounted in a push-pull configuration. One membrane was activated, and the other acted as a counter-balancing spring. The actuation signal was 2.5 kV at 30 Hz, and more

than 3 million cycles were demonstrated without change in the actuation strain or damage to the electrodes [58].

This technology has been developed by the Danfoss group in Denmark in collaboration with RISØ DTU. In July 2008 a separate entity, Danfoss Polypower A/S,[3] has been founded to further develop this process, and to manufacture DEAs with corrugated electrodes on a large scale. Danfoss Polypower were the first to manufacture in high volume an electrode-coated DEA material. They have developed custom machinery that enable roll-to-roll production of hundreds of meters of DEA membranes, from the corrugated membrane fabrication to the lamination of two films to form a capacitor [59]. The electrodes are deposited by a roll-to-roll vacuum sputtering process, which follows the delamination of the membrane from the mould, whose profile height and period are respectively 4 μm and 10 μm. Plasma treatment is used to promote the adhesion of the metal on the elastomer prior to the metallization. The infrastructure allows the coating of different metals, and a roll-to-roll masking mechanism can be used to pattern the electrode, if needed. Recent research effort for the optimization of the corrugation profile has lead to metallized membranes capable of sustaining a strain of 80 % without inducing damages to the metallic layer, by using a mold profile with a 1:1 height over period ratio [60]. The authors have computed an experimental "compliance factor" describing the stiffness of the coated membrane in the compliant direction, and estimated that the new profile is about 4.5 times more compliant than the previous one, which should lead to a strain gain for the same applied electric field when use in a DEA configuration. According to their model, the corrugated metallic electrode with this new profile is 8100 times more compliant than the same metallic film deposited on a non-structured (i.e. flat) membrane.

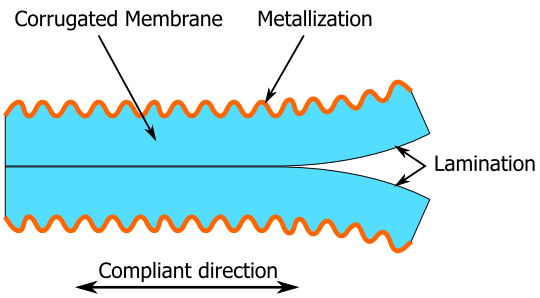

Fig. 12 Corrugated membrane with thin-film metallization applied on the corrugated surface. The sandwiched configuration necessary to make dielectric elastomer actuators is obtained by laminating two metallized membranes back to back

[3] http://www.polypower.com.

Push actuators named *InLastor* were fabricated by rolling the DEA membrane in a cylinder of many layers. With 2500 V actuation (∼31 V/μm), the actuators exhibit a 3 % linear strain, a blocking force of 6 N/cm^2 and a response time below 10 ms [59].

4.4 Patterning methods for metallic thin-film electrodes

One of the main advantage of using metallic thin film as electrode material is the ability to precisely define the shape of the electrode via different methods of patterning (Fig. 13). The three techniques compatible with elastomer membranes are as follows.

Shadow masking A shadow mask can be used to selectively expose the surface of the elastomer during the coating process, similar to what can be done with carbon-based electrodes. Laser cutting of thin (<100 μm) steel sheets can be used to obtain structures down to ∼100 μm. Smaller structures, down to a few micrometers, can be achieved through the use of a microfabricated stencil [61]. Using focused ion-beam milling for the fabrication of the stencil, deposition of metallic structures smaller than 100 nm has been demonstrated [62]. But the fabrication process of nano-stencil is quite complicated and expensive.

The patterning steps (Fig. 13(left)) involve (a) the application (and alignment, if needed) of the shadow mask on the membrane, (b) the deposition of the metal film and (c) the removal of the mask. The main advantage of this technique is its rapidity due to the possibility of re-using the masks. The disadvantages include the contact of the mask with the dielectric membrane, and the shape limitation (i.e. the difficulty of patterning closed paths such as a ring). Lacour

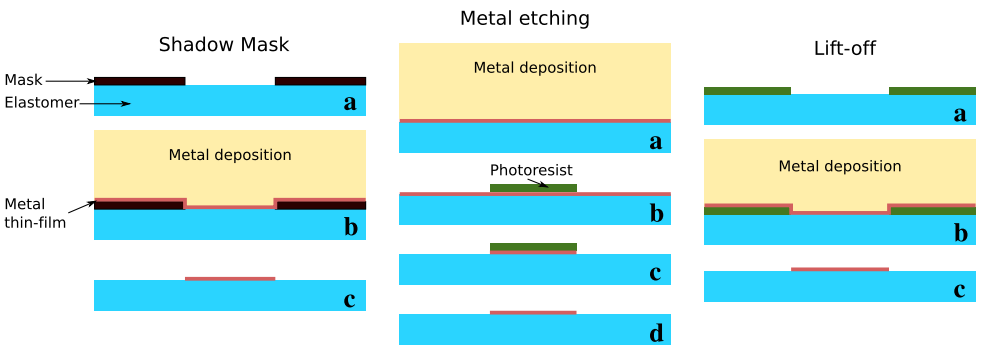

Fig. 13 The three principal methods to pattern metallic thin films: Shadow masking (*left*), blanket deposition followed by a photolithography and a metal etch (*center*), and lift-off (*right*)

et al. have used shadow mask made in a polyimide foil to define conductive stripes on a silicone substrate [63], and the Danfoss Polypower metallization process can be used in conjunction with a roll-to-roll shadow mask [59].

Metal etching Photolithography combined with metal etching is another possibility (Fig. 13(center)). It consists of depositing a blanket metal electrode on the elastomer (a). A thin photoresist layer is then applied on the metal and patterned to selectively protect the metal layer (b). This step is followed by the etching of the exposed metal (c), and finally the photoresist is stripped from the metal (d). This process, which is the standard patterning method used in the integrated-circuit (IC) industry, has been successfully demonstrated to pattern metallic electrodes on elastomeric membranes for DEA applications by several authors [9, 27, 50, 53, 64]. Compared to the shadow mask process, any shape can be realized with photolithography, and features with size down to 5 µm have been demonstrated on soft polymers [9]. However, the number of steps and the required processing time are higher than for the shadow mask process.

Lift-off Another patterning possibility using photolithography and requiring a reduced amount of steps is the lift-off process (Fig. 13(right)). A layer of photoresist is applied and patterned on the elastomer membrane (a). Unlike the metal-etch case, the exposed zones of the membrane after the development of the resist are the regions that need to be coated. The metal is then deposited over the patterned photoresist (b). Finally, the metal-covered resist is stripped in solvent, leaving the patterned metallic electrode on the elastomer (c). The lift-off process has been successfully used to pattern metallic layers on soft elastomers [55, 65–67].

Photolithography on silicone membranes Conventional recipes for photolithography involve pre- and post-bakes of the photoresist at high temperature, which must be avoided with a silicone substrate because of the risk of generating cracks in the metallic and photoresist layers due to the difference in the coefficient of thermal expansion (CTE) between the elastomeric membrane and the photoresist. A specific process for photolithography on soft elastomer must be developed, as stated by Pelrine et al. without giving details regarding their method [9]. A few authors have published specific information on their photolithographic process on silicones, whose focus is mainly aimed towards avoiding the formation of cracks in the resist caused by the expansion of the silicone layer. For example, Pimpin et al. have placed the photoresist-coated substrate in a desiccator at room temperature for 12 hours in order to remove the solvent from the resist, instead of the traditional hot-plate or oven baking [50]. Some research groups have used the negative photoresist SU-8 to pattern structures on a silicone layer, because it is stronger and has a much larger coefficient of thermal expansion compared to conventional resists, thus avoiding the formation of cracks during the process [65–67]. Because SU-8 is an epoxy, it can therefore not be stripped in solvents after cross-linking, and the SU-8 mask must therefore be mechanically peeled off from the substrate. This imposes limitation on the mask design, as the crosslinked SU-8 must form a continuous single part. Guo and DeWeerth have solved this limitation by using an intermediate sacrificial layer: a water-soluble poly(acrylic acid) (PAA) was coated directly on the PDMS, the photopatternable SU-8 being then spun on top of it. The PAA layer is dissolved in water as a last step, to allow the stripping of the SU-8 mask [65].

In addition to CTE mismatch-induced cracking of the photoresist layer, the proper wetting of the silicone surface by the photoresist and the adhesion thereof represent another challenge, due to the extremely low surface energy of silicone. Consequently, standard novolak-based resists have a tendency to dewet when directly applied on silicone, which is the case in the lift-off process. To address this issue, Maghribi et al. have used oxygen plasma activation (1 min at 100 watts with an oxygen flow of 300 sccm) just before spin-coating the resist, in order to increase the surface energy of PDMS and ensure proper wetting by the photoresist [56]. Diebold and Clarke present another approach with the use of a mixture of Polydimethylglutarimide (PMGI) and standard Novolak resist, as PMGI was shown to present a good adhesion on silicone [68].

4.5 Interconnects

Depending on the targeted application and required output strain, metal thin-film electrodes may have too large a stiffening effect on the elastomer membrane, even when applied with one of the methods described above. There are therefore situations for which carbon electrodes would be more suited. However, one of the main advantage of metallic electrodes are their high conductivity and ease of patterning down to the micrometer scale. Even for actuators which would require a highly compliant active zone made with a carbon-based electrode, compliant metal thin films can be used as interconnect to bring the electrical signals from the actuator's frame to the active zone. Long and narrow tracks with a low electric resistance can be patterned on the dielectric and used as soft interconnects, which is not feasible with carbon electrodes: in addition to the difficulty of patterning small structures, a narrow and long interconnect made with a material having a surface resistance in the tens of kΩ/□ range is not realistic.

The important parameters of interconnects are (a) a high conductivity and (b) the ability to be repeatably stretched without damage. The stiffening effect on the membrane is

of secondary importance. In addition to the three types of thin-film electrode presented above (patterned electrodes, buckled electrode and corrugated electrodes), there are a few other technologies that can be used for interconnects, while having a too large stiffening impact to be used as active electrode in a DEA. For example, several authors reports on large uniaxial strains (up to 30 %) obtained with metallic thin films deposited on a flat elastomeric substrate, greatly exceeding the usual 3–4 % yield strain of metals [64, 69]. The authors have discovered that microcracks are created in the strained metallic tracks. As these cracks do not propagate completely across the track, a conduction path is conserved up to large strains. It is difficult to evaluate the importance of the deposition parameters and of the stretching profile (very small increments with long pauses between each steps [64, 69]) on the elongation at break for metallic thin films. As a comparison, we have previously strained sputtered gold layers on PDMS at a constant speed and observed loss of conductivity for strains as low as 3 % [70].

5 Novel techniques for compliant electrodes

In addition to the two mainstream types of electrode (carbon and metal thin films) described in the previous sections, some research groups have worked towards developing new types of compliant electrode for DEAs, in order to progress towards the perfect electrodes for DEAs combining compliance with ease of patterning, or to develop new useful features such as self-clearing in case of dielectric breakdown. This section presents some of the emerging and exotic methods to make compliant electrodes for DEAs and pinpoints the advantages compared to the more conventional methods.

5.1 Implantation of metallic nanoclusters

Carbon powder electrodes are extremely compliant because they are formed by nano/micro particles that can slide relative to each other when the elastomeric membrane on which they reside is stretched. However, their adhesion to the membrane is extremely weak, making them messy and unreliable. On the other hand, metal thin films present a much better adhesion but lack compliance. Implantation of metallic nanoclusters at low energy takes the best of the two worlds by creating metallic nanoparticles in the first tens of nanometers below the elastomer surface (Fig. 14(a)–(b)). These metallic clusters can move relative to each other, thus forming an electrode much more compliant than a plain thin film, and because they are located inside the elastomer matrix, the adhesion and resistance of these electrodes is excellent.

Two different implantation methods leading to the formation of metallic nanoclusters into PDMS have been presented in the literature: Filtered Cathodic Vacuum Arc (FCVA) implantation [70–74] and Supersonic Cluster Beam Implantation (SCBI) [75].

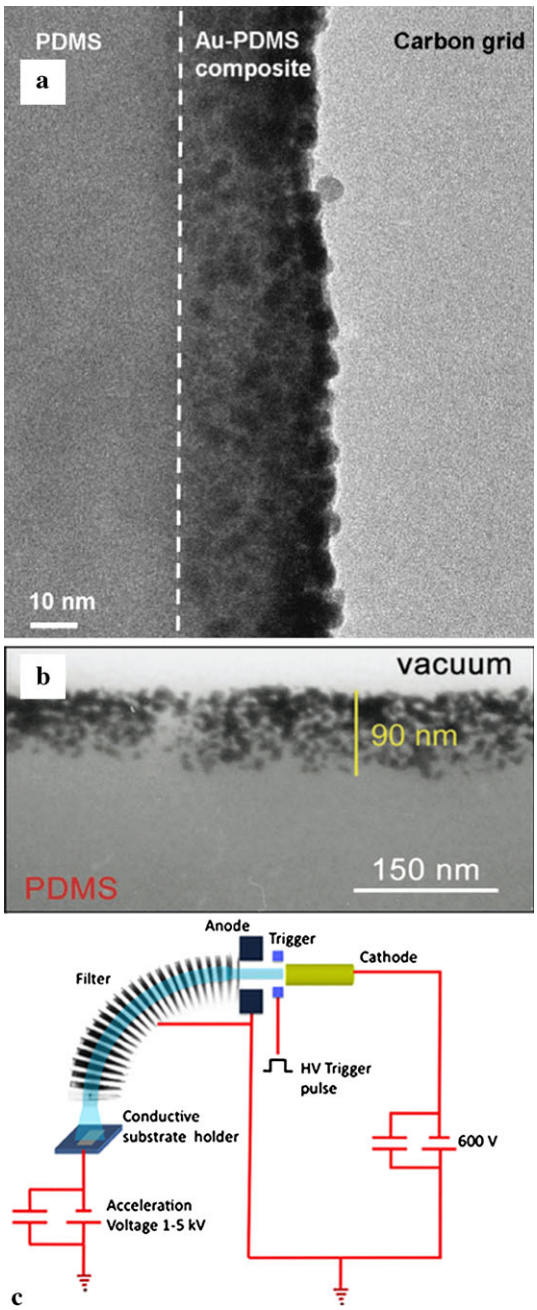

Fig. 14 (**a**) TEM cross-section of Au nanoclusters implanted by FCVA into PDMS with an energy of 10 keV and a dose of 1.5×10^{16} at cm^{-2}. From [74] ©2010 Elsevier ltd. Reproduced with permission. (**b**) TEM cross-section of a Au/PDMS nano-composite obtained by SCBI for an equivalent thickness (i.e. thickness obtained when depositing on a hard substrate) of 35 nm (exact dose unknown). From [75], ©2011 WILEY-VCH Verlag GmbH & Co. Reproduced with permission. (**c**) Schematic representation of the FCVA implantation process: the high density plasma is created by a high-voltage pulse that vaporizes the cathode material. A 90° bent solenoid filters the plasma by trapping the large, heavy macroparticles. From [74], ©2010 Elesevier ltd. Reproduced with permission

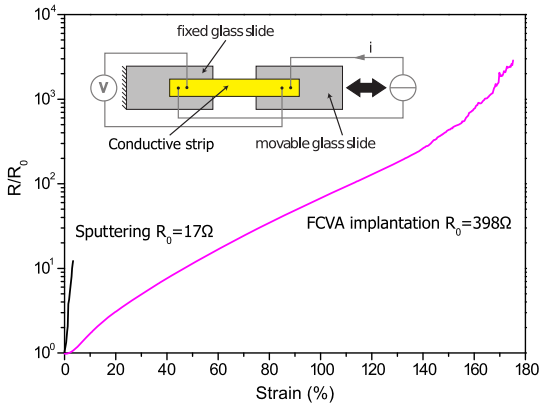

Fig. 15 Change of resistance versus strain for a gold-sputtered and a gold-implanted strip up to the damage threshold. The sputtered layer can only sustain a few percent strain whereas the implanted strip can be stretched up to 175 % before losing conductivity. From [70], ©2009 WILEY-VCH Verlag GmbH & Co. Reproduced with permission

Filtered cathodic vacuum arc In FCVA, a plasma is generated between the cathode (the metal to be implanted) and a counter electrode (anode) by a high-voltage pulse that vaporizes the cathode material (Fig. 14(c)). The plasma, consisting of electrons, metal ions and large, undesirable particles is then filtered by a magnetic filter to remove the macroparticles [76]. The metal cations are finally accelerated towards the target by an electric field. Our group has worked extensively on low energy (2–10 keV) FCVA implantation of titanium, palladium and gold ions into PDMS targeted at the fabrication of compliant electrodes for DEAs. Our investigation of gold-implanted PDMS have shown a percolation threshold of about 1.5×10^{15} at/cm^2, leading to reasonably low surface resistance ($\sim$1 k$\Omega/\square$), large stretching capabilities while remaining conductive and low impact on the Young modulus of the silicone membrane [70]. Conductive strips were implanted with gold on a silicone membrane and stretched. The resistance versus strain was measured with a four-points setup. Strains of up to 175 % were observed before the electrode was damaged, which is much larger than a gold-sputtered strip of identical size (Fig. 15). The implanted layer extended from the surface to a depth of 20–30 nm depending on acceleration energy. The Young modulus of this ultra-thin implanted layer was measured to be 0.2–5 GPa depending on energy and dose, much lower than the Young modulus of bulk gold [74]. When used to make electrodes on a 25 µm PDMS membrane whose initial Young's modulus is 1 MPa, ion implantation creates a 100 % relative increase of the stiffness, which is much lower than the impact of a plain evaporated thin film of comparable thickness. Gold-implanted tracks were cyclically stretched to 20 % without degradation [70].

Circular buckling DEAs with FCVA gold-implanted electrodes were fabricated and characterized [73, 77]. They exhibited vertical displacement over diameter ratios up to 25 %, which is 4.5 times higher than a similar actuator made with patterned thin-film electrodes (cf. Sect. 4). FCVA implantation is particularly interesting for the fabrication of compliant electrodes: First, the low energy limits the penetration depth of the ions into the elastomer, and allows percolation at low doses. The low energy also limits the collision-induced damage at the surface of the elastomer which contributes to stiffen the polymer (carbonization, broken bonds, etc.). Secondly, the high ion flux allows obtaining a conductive layer in a short amount of implantation time (a few minutes).

Supersonic cluster beam implantation In plasma assisted SCBI, the metal is vaporized in the same manner as with FCVA, but the plasma is subsequently quenched by a pulse of inert gas and it condenses to form neutrally charged clusters. The clusters are then injected into the deposition chamber where they impact the target [78]. With this technique, neutral atoms are implanted and charging of the elastomer surface is therefore avoided. Corbelli et al. have used this method to create electrodes composed of conductive gold clusters into PDMS [75]. Even if the energy per atom is low ($\sim$0.5 eV/at), whole clusters consisting of several thousand of atoms are reaching the target, and their kinetic energy is large enough to penetrate about 100 nm into the PDMS [75]. Using this method, Corbelli et al. obtained electrodes with a very low surface resistance (about 100 $\Omega/\square$) for an unspecified atom dose (180 minutes of implantation were necessary, which makes it a slow process). The conductive tracks were stretched up to 100 % while remaining conductive. The upper limit was defined by the mechanical failure of the elastomer, and not by the electrode ceasing to conduct. Cyclic stretching to 40 % for 50000 cycles showed a decreasing variation of the resistance change between the two extreme positions with the number of cycles. Because the authors of this study are not targeting DEA application specifically, they have not characterized the Young modulus increase caused by the implantation, but as the technique is very similar to FCVA implantation, a comparable impact should be expected. Indeed, TEM cross-sections of FCVA [74] and SCB [75] implanted silicone look similar, but with much larger clusters and penetration depth in the case of SCBI, probably due to the higher kinetic energy of the clusters for SCBI (Fig. 14(a)–(b)).

Patterning methods for metallic nanoclusters electrodes Similar to metallic thin films, implanted metallic clusters can be patterned with the techniques presented in Sect. 4.4: shadow masking and photolithography. In the latter case, only the lift-off process can be used. It is indeed not possible to selectively remove the clusters with a metal etchant, as they are implanted and thus below the surface. Using shadow masking, our group has fabricated an array of

$100 \times 100\ \mu m^2$ actuators for single cell stretching that are capable of deformation up to 80 % actuation strains [79], thus demonstrating that implanted electrodes can be patterned on the micron-scale while being much more compliant and presenting a better adhesion to the substrate compared to their thin-film cousins. The process of creating metal clusters electrodes is similar to that of depositing metal thin film by evaporation or sputtering in terms of involved equipment (vacuum chamber) and process flow. However, metal cluster electrodes have the advantage of being intrinsically compliant without the need of a special membrane microstructure (cf. Sect. 4.3), prestretching (cf. Sect. 4.2) or patterning of the electrodes (cf. Sect. 4.1), as necessary for metal thin films. Furthermore, unlike corrugated and buckled electrodes, metal cluster electrodes are compliant in the two in-plane directions, hence placing no restriction on the strain direction. Implanted metallic cluster electrodes are thus representing a progress towards metallic compliant and patternable electrodes for DEAs.

5.2 Photopatternable electrodes

Patterning of the compliant electrodes presented up to now was always made extrinsically, with the help of stencils or photoresists. However, intrinsically patternable compliant electrodes are very desirable, for they can greatly simplify the structuring process. Delille, Urdaneta et al. have reported on photosensitive electrodes based on platinum salts mixed in a photosensitive elastomer (Loctite 3108) [80–82]. The ingenuity of the process resides in the use of a filler (Pt salt) which is transparent to UV light. Indeed, previous attempts to produce a photopatternable conductive elastomer by mixing conductive fillers in a photosensitive elastomeric matrix were not conclusive because of the absorption and the scattering by the filler particles of the UV light needed for the cross-linking [81].

The elastomer-salt composite is applied on a substrate and exposed to UV light through a mask to locally induce cross-linking of the loaded elastomer, and the uncrosslinked elastomer is then subsequently flushed away in acetone. The composite is then immersed into an aqueous reducing solution, causing the Pt salt to diffuse to the surface, reducing to the metal at the polymer/liquid interface (Fig. 16). The percolation threshold is observed for 6–7 % vol Pt salt at which point the surface resistance of the electrode is $\sim$200 $\Omega/\square$, and it drops down to 2.2 $\Omega/\square$ for 15 % vol [80]. The Young modulus of the composite is shown to be unaffected by the quantity of filler and remains close to that of pure Loctite 3108 (10 MPa) [82]. However, the stiffness of the photosensitive elastomer used in this study is one order of magnitude higher than elastomers commonly used for DEAs, and direct comparison with the stiffening effect of the other kind of compliant electrodes is not possible. For an application as

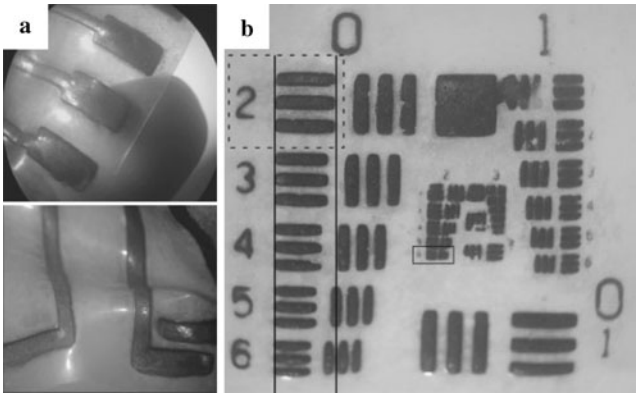

Fig. 16 Photopatternable and stretchable platium salt electrodes on elastomer [80] ©2007 WILEY-VCH Verlag GmbH & Co. Reproduced with permission

compliant electrodes for DEA, the Loctite 3108 elastomer should be replaced by an UV-sensitive low-durometer silicone, such as the SEMICOSIL 945 UV (Wacker, Germany).

Patterned structures down to 350 µm were obtained with the Loctite 3108/Pt salt compound, whereas a resolution of 310 µm was observed for pure Loctite 3108. The slight decrease in resolution in presence of the salt is attributed to light scattering [80]. These electrodes can be stretched up to 150 % before losing conductivity and have been cyclically stretched up to 30 %, at which point mechanical failure occurs after about 1000 stretching cycles. For smaller strains, a degradation is observed during the first hundreds of cycles, but it then stabilizes. The mechanical and electrical properties of these electrodes depend on the content of Pt salt, which was varied between 9 and 14 %.

The downside of this pioneering method, although intrinsically patternable, is its relatively poor resolution compared to the previously mentioned techniques, such as stencil, or photolithography.

5.3 Self-clearing electrodes

One of the principal failure mode of DEAs is electrical breakdown of the dielectric membrane due to an excessive electric field applied between the electrodes. The global electric field is equal to the applied voltage divided by the average thickness of the membrane. However, the electric field can be locally higher, for example because of defects in the membrane. When breakdown occurs, a current flows through the membrane at the location of the defect. The consequence of breakdown is usually a permanent conductive carbon track being created through the membrane, effectively short-circuiting the electrodes, and thus preventing the actuator to charge and move. Depending on the current output capability of the source used to drive the actuator, breakdown can also cause puncture of the membrane, which

may result in the complete tear thereof, depending on the tear strength of the elastomer.

Self-clearing electrodes can greatly increase the lifetime of DEAs by being able to survive a certain amount of localized breakdowns. This effect is well known to the film capacitor industry: the extremely thin metal layer forming the electrodes vaporizes around the defect upon breakdown, effectively insulating the short-circuited zone from the electrode.

Single-walled carbon nanotubes In the field of DEAs, Yuan et al. have observed self-clearing on electrodes made with single-walled carbon nanotubes (SWCNT) [83, 84]. They tested actuators that were made from an acrylic elastomer (VHB 4905) prestretched biaxially by 200 % and with two types of electrode: carbon grease and SWCNT. They applied a 3 kV signal between the electrodes and mechanically punctured the membranes in the active area with a wood pin. After the damage was inflicted, the actuators with carbon-grease electrodes exhibited no strain when activated and behaved resistively (drawing a current proportional to the voltage input). The actuators with SWCNT still behaved like capacitors after the damage, drawing current only when the voltage changed, and their strain amplitude was reduced from 100 % to 80 %, a value corresponding to the area of the electrodes that was cleared by the defect.

The downside of these SWCNT electrodes is that, similar to the case of loose carbon black, they are not physically bound to the dielectric membrane (unless the adhesive VHB acrylic elastomer is used as membrane material). In addition, the handling and patterning difficulties of carbon-based electrodes also concern SWCNT, which are therefore not the best candidate for miniaturization and mass fabrication, without mentioning the prohibitive cost of carbon nanotubes.

It is because conductive SWNT electrodes are extremely thin (5–250 nm for surface resistance of 20–0.1 k$\Omega/\square$) that they exhibit self-clearing capabilities while carbon-grease electrodes do not. Consequently, self-clearing is also expected from the different metal thin-film electrodes (cf. Sect. 4) if the deposition parameters are carefully chosen, similar to the case of film capacitors.

Other self-clearing compliant electrodes Self-clearing of compliant electrodes on elastomers has also been observed and characterized with electrolessly deposited silver, a method to deposit thin silver layers from liquid precursors [85]. This technique is normally used to apply the reflective coating on mirrors, and has recently been applied to the fabrication of compliant electrodes for DEAs [86]. The initial resistance of these electrodes is extremely low (3–5 $\Omega/\square$), and upon stretching, microcracks are formed on the layer, similar to what was observed for some standard thin-film metallic electrodes (cf. Sect. 4.5). Upon localized dielectric breakdown, the metallic layer is thin enough to be vaporized around the defect [85, 86]. These electrodes were shown to sustain uniaxial strains of 10 % while remaining conductive. This electrode technology has been applied to the fabrication of bending uni- and bi-morph DEAs, a configuration in which the electrode is not strained much [85, 86]. In the more conventional surface strain configuration, Low and Lau reported actuation surface strains up to 21 % (10 % linear) with electrolessly deposited silver [87]. Self-clearing was also reported for doped conductive polymer electrodes made with poly(3-dodoxylthiophene) or polyaniline nanofibers [83, 88].

Even though the self-clearing process can electrically save the membrane from permanent damage by clearing the electrodes, a breakdown can also cause dramatic mechanical failure, depending on the elastomer used as membrane. A tiny defect in a prestrained membrane made from a low tear-strength silicone will at once propagate and destroy the membrane. In summary, the ability of a DEA to self-heal in case of localized breakdown depends on a combination of factors, such as the electrode type, the material used as membrane, and the current delivered by the voltage source driving the actuator. A careful choice of these three parameters can lead to more robust actuators with increased lifetime.

5.4 Transparent electrodes

Conductivity and compliance are two necessary requirements for DEA applications which characterize all of the electrode types presented in the previous sections. Some electrodes present additional interesting characteristics, one of them being partial transparency, which opens the door to optical applications. Kovacs and Düring report the fact that extremely thin layers of loose carbon black smeared on an adhesive acrylic elastomer membrane are semi-transparent but quantified results are not provided [36]. Transparency is also reported by Hu et al. for carbon nanotubes sprayed on acrylic elastomer membranes [89]. In actuator configuration (i.e. two electrodes), they report a transmission in the visible domain between 25 % and 40 % at 0 V. The transmission increases with increasing voltage and area strain, to reach 40 % to 50 % at 2.7 kV. The carbon nanotubes electrodes from Hu et al. sustained up to 700 % strain when uniaxially stretched, which represents the largest stretch under which a conductor has remained conductive [89]. Gold and palladium implanted electrodes also presents partial transparency with values between 35 % and 70 % for a single electrode, depending on the metal and the implanted dose [70]. Finally, silver nano-wires (AgNW) are also reported to be partially transparent by Yun et al. with transmission in the visible range between 45 % and 80 % depending on the

surface density of the nano-wires [90]. In addition to their transparency, AgNW electrodes can also sustain high current density and have been used as electrodes for Joule heating [90].

The transmission values mentioned for these different compliant electrodes are highly dependent on the quantity of conductive material applied on the membrane. Better transmission is achieved with as little electrode material as possible, which can have a negative impact on the maximal strain at which the electrodes lose their conductivity, and consequently limit their actuation strain. Shian et al. have studied the relation between the optical transmission and the achievable actuation strain for SWCNT and AgNW at different surface densities [91]. Through the use of a figure of merit, they showed that SWCNT outperformed AgNW, with an optimal transmission of 91 % leading to an area actuation strain of 190 %.

Transparency, even partial, of compliant electrodes opens a new range of potential applications, such as flexible screen with haptic feedback or adaptive optics. However, due to the light scattering induced by the particles forming the transparent electrodes [89], very demanding applications such as imaging are not realistic. In this situation DEA-based optical systems are more likely to keep the electrodes out of the optical path, such as for the tunable lens from Carpi et al. which consists of an annular electrode encircling the optical zone [92].

6 Discussion

Because of their high energy density and large strains, DEAs present characteristics unmatched by any other kind of mainstream actuators (electromechanical, piezoelectric, thermal, etc.), and their ability to hold a position without drawing current (if one neglects the small leakage current through the dielectric) makes them attractive for a broad range of battery-powered consumer applications. On the other hand, their 0.3–4 kV driving voltage can be an impediment to commercialization due to the size and efficiency of the driving electronic circuit.

A large part of the research effort of the EAP community has been targeted towards the optimization and characterization of the elastomeric membrane. Different types of elastomer, their non-linear stress-stretch relationship, breakdown strength, dielectric constant, viscoelasticity, and processing methods have been studied in detail, as they are key parameters that impact the performance of the actuator. However, the compliant electrodes play an equally important role relative to the actuator performance, a fact that has been unfortunately partially neglected by groups working on DEAs. Quickly applied and extremely compliant, carbon powders and greases are practical to rapidly produce macroscale demonstrators, but their limited lifetime and reliability make them an unsuitable choice outside a research laboratory environment.

Because of the many practical applications which would benefit from the use of DEA structures encompassing a large spectrum of sizes and operational conditions, there is no unique compliant electrode technology that emerges as the ideal solution. In the following paragraphs, we will examine some of the potential uses of DEAs and the implied requirements on the compliant electrodes.

6.1 Miniaturization

Miniaturized DEAs are of particular interest due to their large actuation strain compared to other microactuators, and envisaged applications include Braille displays [93, 94], biological single cell stretching [79], microfluidic pumps [40], localized haptic feedback [94], etc. The key requirements for compliant electrodes in small-scale applications include ease of patterning, and compatibility with microfabrication processes and clean-room environment. With respect to these criteria, metal thin-film electrodes (Sect. 4), implantation of metallic nanoclusters (Sect. 5.1), and platinum salt electrodes (Sect. 5.2) are the best suited methods. If large strains (i.e. minimized stiffening impact) and biaxial strain is required, then metal implantation is the best compromise. Using this method, our research group demonstrated up to 80 % strain on patterned $100 \times 100\ \mu m^2$ actuators [79]. This is one of the smallest reported DEA to this date, and the large obtained strain shows the low stiffening impact of low energy metal ion implantation.

The ability to precisely pattern mm- or μm-size electrodes allows the fabrication of arrays of actuators on a single membrane, either electrically independent or connected. This can be used to fabricate devices which are not necessary small, but which are formed by a collection of miniaturized electrodes, such as tunable gratings [43], arrays of single cell stretchers or Braille displays.

6.2 Towards low actuation voltages

The reduction of the driving voltage is an important objective for the widespread use of DEA-based devices in consumer goods. Indeed, DEAs are potentially energy-efficient devices, capable of large work output compared to their size and weight, but at this time, they unfortunately require DC-DC converters and heavy-duty switching transistors for the generation of the high-voltage driving signals. Even though some companies are already selling small-scale DEA-based products, such as a haptic feedback device for iPod Touch using the ViviTouch[4] technology developed by Artificial

[4] www.vivitouch.com.

Muscles Inc, or a Laser speckle reducer from Optotune,[5] there is still much room for improvement. Instead of a bulky add-on, the future of the ViviTouch device will be a direct integration inside small portable devices such as smartphones, whose next generation could also contain laser-pico projectors with DEA-based de-speckler using Optotune's technology. The Schlaak group, using its stack fabrication technology (cf. Sect. 3.1) developed a vibrotactile display for mobile applications such as a portable media player, giving haptic feedback to the user [95]. They designed a battery-powered electronic circuit that generates the control signals (up to 1.1 kV) for the actuators, in order to make the device truly independent and portable [96]. However, because of the driving voltage is still over 1 kV, and even though tremendous effort has been made to reduce its footprint, the electronic circuit is still very large and the device (haptic feedback actuator and controlling electronics) is larger than a complete commercial portable media player.

Direct integration of DEAs into consumer electronic products puts tough requirements on the power and size of the driving electronic. Reducing both of these inevitably requires the use of lower voltages. There are several possibilities to decrease the actuation voltage while keeping the output strain constant:

- The use of an elastomeric membrane with a lower Young modulus. However, soft silicones tends to exhibit a strong viscoelastic effect, have a reduced breakdown strength, and generate less force.
- The use of an elastomeric membrane with a higher relative permittivity to increase the device's capacitance. Several research groups have attempted to disperse nanoparticles (titanium dioxide, $BaTiO_3$) or dipole molecules into silicones in order to increase the permittivity of the elastomer [97–99]. However, the increase of the permittivity often comes at the cost of a reduced dielectric breakdown field.
- The use of thinner elastomeric membranes which also increases the capacitance of the device, and therefore reduces the voltage needed to generate the electrostatic force. This solution presents the advantage of having no impact on the intrinsic material properties of the elastomer (Young's modulus, viscoelastic behavior, elongation at break, dielectric strength, etc.). The loss of output force can be compensated by using a multilayered actuator.

Reducing the thickness of the membranes places tougher requirements on the electrodes regarding compliance. In the case of the linear material model approximation valid for small deflections, the voltage induced thickness strain s_z for a DEA under free boundary conditions is defined by

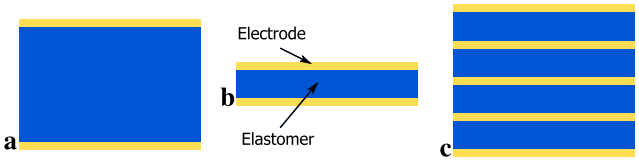

Fig. 17 Schematic representation of the effect of the thickness of the elastomer layer on the stiffening impact of the electrode. (**a**) A DEA made with a relatively thick dielectric layer, which has a high driving voltage. (**b**) The thickness of the elastomer is reduced by a factor of 4 in order to reduce the driving voltage. (**c**) To compensate for the force decrease due to the thinner dielectric, it is possible to stack four layers on top of each other. The ratio of electrode material over dielectric material is higher for case (**b**) and (**c**) than for case (**a**)

Eq. (1). It is therefore expected that an actuator with a membrane twice thinner would require half the driving voltage to achieve the same strain level. The situation is unfortunately more complex, as Y does not represent the Young modulus of the membrane alone, but that of the sandwich formed by the elastomer/electrodes composite. Considering a 3-layers DEA stack (electrode/elastomer/electrode), the effective Young's modulus for in-plane deformation (i.e. isostrain) is given by the Voigt model [100]:

$$Y_{\text{eff}} = \frac{Y_p t_p \cdot 2 Y_e t_e}{t_p + 2 t_e}, \tag{3}$$

where Y_{eff} is the effective Young's modulus of the composite, Y is the Young modulus, t the thickness, and the indices p and e respectively refer to the polymer and the electrode. (The equation is not valid for the out-of-plane buckled electrodes (Sects. 4.2 and 4.3): because these electrodes flatten without being strained, the isostrain condition is not met, and this is precisely the reason why these electrodes are compliant while a flat metallic thin film is not).

When scaling down the thickness of the dielectric layer, it is reasonable to assume that the thickness of the electrodes is not going to change, as it is linked to their fabrication process and already kept at the minimal value necessary to obtain the desired surface resistance. Consequently, the thinner the membrane, the more crucial the need for ultra-compliant electrodes, as the stiffening effect of the electrodes becomes more dominant. This effect is illustrated in Fig. 17: to reduce the driving voltage of a relatively thick actuator (a), the thickness of its dielectric is reduced by a factor of 4 (b). Because the thickness of the electrodes is linked to the fabrication process, it remains unchanged. The ratio of electrode thickness over membrane thickness (t_e/t_p) increases, which causes an increase of the Young modulus of the sandwich in case the electrodes are not perfectly compliant (Eq. (3)). This is also the case if four layers are stacked on top of each other to compensate for the loss of output force due to the decreased membrane thickness (c). For a constant electric field, the output strain of configuration (b) and (c) is smaller than for situation (a).

[5] www.optotune.com.

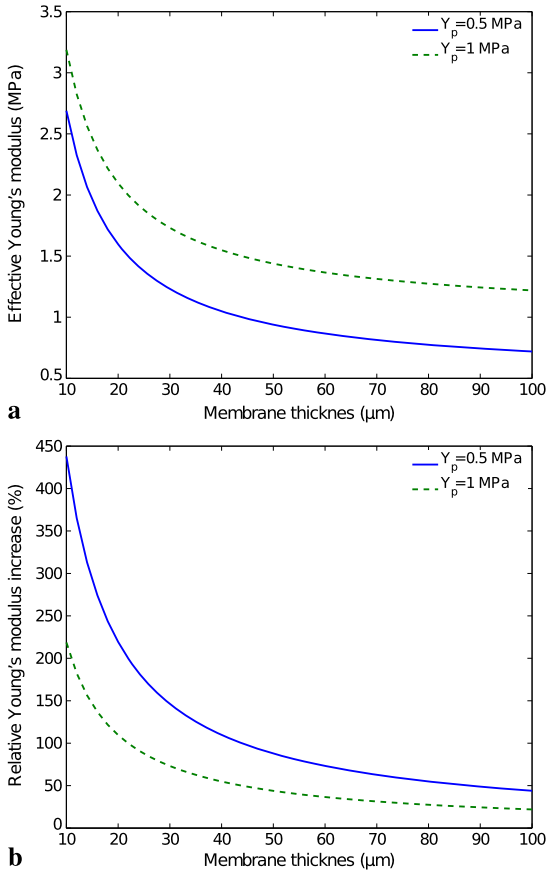

Fig. 18 Computation of the stiffening effect of two gold electrodes (one on each side of the membrane) made by metal ion implantation on elastomeric membranes with a Young modulus of 0.5 and 1 MPa as a function of membrane thickness. The implantation is assumed to be made with an energy of 2.5 keV, leading to an ion penetration depth of 20 nm, and a Young modulus of the implanted composite of 550 MPa in the region with gold ions. (**a**) Resulting effective Young's modulus of the actuator (**b**) Relative increase of the Young modulus compared to the non-implanted elastomer

As an example, let us take a 50 µm-thick PDMS membrane with a Young modulus of 1 MPa, on each side of which a gold-implanted electrode is made (assumed penetration depth: 20 nm and Young's modulus of the implanted layer: 550 MPa for an implantation energy of 2.5 keV [74]). Using Eq. (3), one obtains an equivalent Young modulus of 1.44 MPa, corresponding to a moderate stiffening effect of 44 %. Now if the dielectric membrane is scaled down to 10 µm and implanted with the same parameters, the resulting Young modulus would be 3.2 MPa (stiffening of 220 %), thus showing the crucial role that the stiffness and thickness of the electrodes play in the overall stiffness of the actuator. For this particular example, reducing the membrane thickness by a factor of 4 does not allow to reduce the driving voltage by the same amount to keep the strain unchanged, because the thickness reduction causes a stiffness increase of the actuator sandwich. Figure 18 represents the increased

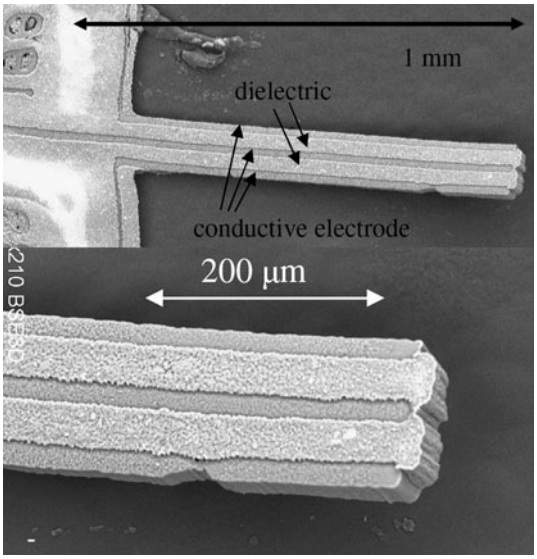

Fig. 19 Miniaturized two layers DEA fabricated by etching grooves into a silicon wafer, which are then subsequently filled with conductive and non-conductive PDMS. At this size scale, the relative thickness of the electrodes becomes important (see also Fig. 17(c)). From [101], ©2011 IEEE. Reproduced with permission

stiffening impact of the electrodes for different membrane thickness in the case of gold implantation, and highlights the increasing impact of the electrodes when the elastomer layer becomes thin.

The preponderant impact of the electrodes for miniaturized devices is also clearly visible on the Bergbreiter's group process (Fig. 19). By subsequent steps of deep reactive ion etching on a SOI wafer and filling of trenches with PDMS, they were able to obtained miniaturized suspended structures in silicon and silicone [102]. They also combined conductive and non-conductive silicone to make thermal microactuators [38] and DEAs [101]. The process is extremely interesting, because it is the closest one to standard MEMS fabrication and it allows the fabrication of stacked actuators with easy access to the electrodes located in the middle. The fabricated 2-layers DEAs were 1 mm long, 40 µm wide and 100 µm thick (5 × 20 µm). In that case, each layer (electrode and dielectric) has the same thickness, which shows how critical the impact of the electrodes becomes when the device's size is scaled down (Fig. 19).

Even though it is possible to produce very thin elastomeric layers (the fabrication of silicone membranes down to 1 µm by spin-coating has been reported [1]), there is currently a lack of an electrode technology that would be compliant enough for such thin-membranes, while meeting the requirements for ease of patterning, clean-room compatibility and large-scale manufacturability. Developing such an electrode would be a key achievement, as it would allow the fabrication of DEAs with an actuation voltage below 100 V.

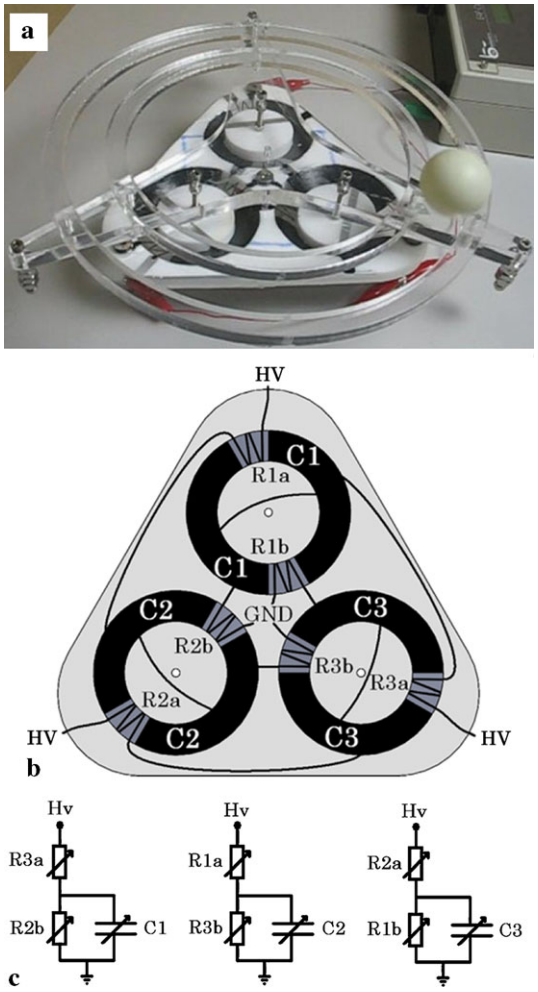

Fig. 20 Ball rolling oscillator based on dielectric elastomer switches. Strain-sensitive resistors are patterned alongside the actuators and are used in a voltage divider configuration to turn the next actuator on and off, thus sustaining an oscillation of the three actuators and allowing the ball to roll along the rail. (**a**) Photo of the finished system. (**b**) Layout of the switches and actuators. (**c**) Equivalent electrical circuit. From [19]

6.3 Integrated sensing

Adding self-sensing to DEAs, i.e. the capability for an actuator to feel its deformation is a necessary step towards smart devices, as it enables feedback control or can give distributed intelligence to a device by incorporating switches and logic gates directly alongside the actuator in the form of a dielectric elastomer switch (DES) [19]. As DES allows the high-voltage switching to be done directly on the membrane (Fig. 20), this considerably reduces the complexity of the driving electronics, and hence its size.

Self-sensing on DEA membranes can be done either resistively by sensing the change in resistance of the electrode while it is being strained, or capacitively by measuring the change in capacitance of the DEA's electrode during actuation. For macro-scale devices capacitive sensing is expected to give more reliable results as it mainly depends on the geometry of the electrode whereas resistive sensing is also very sensitive to the electrode material and its possible degradation with the number of cycles. For miniaturized devices, however, the actuator's capacitance decreases and capacitive sensing becomes almost unusable.

Using resistive sensing for feedback control, or *self-sensing*, puts additional requirements on the electrodes: in order to be able to relate the resistance of an electrode to its deformation, its surface resistance must be well controlled, its degradation with the number of cycle must be limited, and the resistance as function of strain characteristic must not show too large an hysteresis. For smart switches [19], the electrodes must combine the above characteristics with a well controlled coating process allowing to create resistive tracks close to the percolation threshold: when deformed the resistance of a DES much change by several orders of magnitude (from well-conductive to poorly conductive) in order to obtain a switching characteristics. The reader should refer to the review of Anderson et al. for a detailed investigation of DES and self-sensing [11].

Loose carbon powders and carbon-grease electrodes are unsuitable candidates for resistive self-sensing and self-switching beyond the demonstrator stage because of their weak adhesion to the membrane. Metallic thin-film electrodes (either on a corrugated membrane made to buckle out-of-plane) are also not suitable for resistive self-sensing, because their effective length do not change much during actuation and they exhibit therefore a small change of resistance when stretched. Conductive rubber can be used to make electrodes for self-sensing applications, as they combine a high change of resistance when deformed with a good adhesion to the membrane, as well as resistance to wear and abrasion. Furthermore, combined with a patterning method, resistive meanders can be created for effective self-sensing. Electrodes made by metal ion implantation are now also being tested for self-sensing applications and dielectric elastomer switches [103].

6.4 Energy harvesting

A DEA sandwich can be used as actuator (i.e. responding with a mechanical energy output to an electrical input), but it can also function as energy generator, using the change in capacitance to transform mechanical deformation into electrical energy. Prototypes of dielectric elastomer generators (DEG) of different sizes have been built, from a small device integrated to a shoe heel, to large actuators mounted on a buoys for energy harvesting from ocean waves [18, 104, 105].

Although very large deformations exceeding 100 % [4] or even 1000 % [47] have been demonstrated in actuator mode, electrically induced strain in DEAs typically lies around

10 %–50 %, and their electrodes are therefore designed accordingly. In generator mode, the deformation of the elastomer is mechanically induced and consequently mainly limited by the elongation at break of the elastomer, although other important failure modes must be accounted for, such as dielectric breakdown and loss of tension [106]. Generated energy from the deformation of a dielectric elastomer is based on a cycle during which charges are placed at low voltage on a stretched membrane, which is subsequently relaxed. The decrease of capacitance causes a voltage boost and the charges are harvested at a higher voltage [105]. The generated energy per cycle is proportional to the difference of capacitance of the generator between the two states [107], which is linked to the fourth power of strain. A dielectric elastomer generator designed to maximize the output energy per cycle is therefore likely to operate at large strain, within limit of the different failure modes. Because the electrodes are submitted to that same amount of strain, and as they must survive being deformed to this high strain level for a large number of cycles (1000 km for a heel-strike DEG is a little short of 1 million cycles, and 10 years operation of an ocean-wave harvesting device represents about 70 million cycles), the electrodes, and not the dielectric, are likely to be the limiting factor defining the strain at which the DEG can operate.

We have mentioned above that the energy output of a perfect material is increased with increasing strain levels, but the reality is a bit more complex because internal losses degrades the performance of the DEG. For acrylic-based DEGs, Foo et al. have analyzed the impact of mechanical and electrical losses, respectively due to the viscoelasticity of the elastomer and the leakage current through the dielectric [108]. They showed that the performance are highly dependent on the maximal stretch and on the cycle time, and can, in some cases lead to negative amounts of energy being produced. They showed the existence of optimal parameters to optimize the performance, and that these parameters differ depending on the optimization target, namely energy generated per cycle or energy conversion efficiency. For a cycle time shorter than the viscoelastic mechanical and electrical self-discharge time constants of the generator, the energy per cycle tends to increase with strain, while there exists an optimum value for the efficiency. The authors present a practical example of a generator with an initial prestretch of 4 and a cycle time of 4 seconds. Considering deformation up to a final stretch value of 6, they note that maximizing the harvested specific energy implies deforming the generator to its maximal strain, whereas if the goal is to maximize the conversion efficiency, then a stretch of 5 should be used [108]. Assuming that the electrodes are applied to the membrane *after* it is prestretched by the initial factor of 4, the two optimal strains correspond to electrode stretches of respectively 1.5 and 1.25, although for the first case, higher strains would even be better. This strain, although higher than the typical deformation encountered in actuator mode, remains quite moderate and in the range of most of the electrode types presented previously. However, it is crucial that the compliant electrodes survive being stretched by this amount for a large number of cycles.

Unfortunately, there are not many published data on the lifetime of compliant electrodes and their degradation with time. It has been characterized by Urdaneta et al. for their platinum salt electrodes [80] (cf. Sect. 5.2) and by Rosset et al. for gold-implanted electrodes [70] (cf. Sect. 5.1). Both types of electrode show a stable resistance for a strain of 20 %, even though none of them were tested up to 1 million cycles. Both types of electrode show a continuous degradation of the resistance for cycles up to 30 % strain, suggesting that an operation around the maximal efficiency zone should be possible, but the maximal specific energy strain zone (stretch of 1.5 and above) is out of reach.

In addition to their elongation at break and lifetime, the electrical resistance of the electrodes is also an important parameter, as it induces losses. Kornbluh et al. state that the conductivity of the electrodes is of secondary importance because of the high voltage and relatively low joules losses [104], and DEG with carbon-based electrodes have been successfully demonstrated [109–111]. However, for large-scale devices, minimizing the Joules losses becomes important. The company SBM Offshore[6] is developing wave energy converters in the form of long (target: 400 m) tubes in which a traveling wave creates a local deformation [18]. The active sections of the tube consists of a long (150 m) band of Danfoss' corrugated material (cf. Sect. 4.3) rolled into a 60-layers cylinder of 800 mm diameter. The authors note the crucial importance of a low series resistance, and that even when using the metal-covered Danfoss Polypower material, the resistance of their 150 m band was too high if a single localized electrical connection was used [18]. The authors have developed a multilayer connection process that links each layer in parallel, and keeps the overall series resistance of a section lower than 10 Ω.

In addition to the low resistance provided by its metallic electrodes, the Danfoss material presents the advantage of being available in large quantity, which is another requirement for large-scale energy scavenging devices, together with reliability and low cost. The company has recently developed a new optimized corrugated profile with up to 80 % strain in the compliant direction [60], and the replacement of the silver electrode by another metal could reduce the fabrication costs. The downside of the Danfoss material is the directionality of the compliance. Indeed, because the energy generated per cycle depends on the deformation-induced change of capacitance, equi-biaxial stretching is preferable.

[6] www.sbmoffshore.com.

Table 4 Main advantages and disadvantages of the principal types of compliant electrode used for DEAs

Electrode technology	Advantages	Disadvantages
Carbon electrodes (Sect. 3)	Low impact on stiffness	High resistivity
	Cheap and rapidly made	Easily damaged
Metallic electrodes (Sect. 4)	High conductivity	High impact on stiffness
	Patternability	
	Well-adapted to large-scale production	
Novel techniques (Sect. 5)	New specific features	Complex process
		Expensive

In addition, many of the published designs, such as SRI's shoe-heel generator [104], McKay's push-pull self-priming configuration [109, 110] or Kaltseis' balloon [111] involve a biaxial deformation of the membrane and could not be made with the corrugated material. However, SBM Offshore's approach shows that it is possible to design DEG with uniaxial deformation, and alternatively, a method such as the prestretch-induced out-of-plane buckling (cf. Sect. 4.2) could be used to produce metal-based well-conductive electrodes for DEG requiring biaxial deformations. The higher stiffening impact caused by metallic electrodes compared to other technologies causes a reduction of the DEG strain for a given force input, and hence a smaller amount of produced energy per cycle. However, as the electrodes can be considered as purely elastic (compared to the elastomer membrane), they are not dissipating energy, and do not contribute to the mechanical losses. They therefore do not negatively impact the conversion efficiency, and should instead improve it by reducing the electrical losses.

7 Conclusions

The principal properties of the compliant electrodes presented in the previous sections are summarized in Table 4, and the main characteristics of the different variants of carbon black and metallic electrodes are illustrated on Fig. 21 with their strong and weak points indicated with + and − signs respectively.

Compliant electrodes for DEAs are rapidly evolving, and much progress has been made since the first reported devices in 1998 [1]. Ideal electrodes for EAPs would enable large-strain actuation, efficient energy harvesting, with integrated logic or feedback based on self-sensing. Such an electrode combines outstanding compliance (softer than the elastomer, of order 0.1 MPa), low sheet resistance ($<1\ \mathrm{k}\Omega/\square$), is much thinner than the membrane (a few µm or less), readily patterned on the µm scale on the elastomer, has excellent adhesion to the membrane, controllable piezo-resistance, no viscoelastic response, and no change in properties after millions of cycles at strains of over 50 %. To date the majority of research labs have used loose carbon particles or carbon-loaded conductive greases, which are indeed highly compliant but fail to meet most of the other criteria. Ingenious methods have been developed based on standard

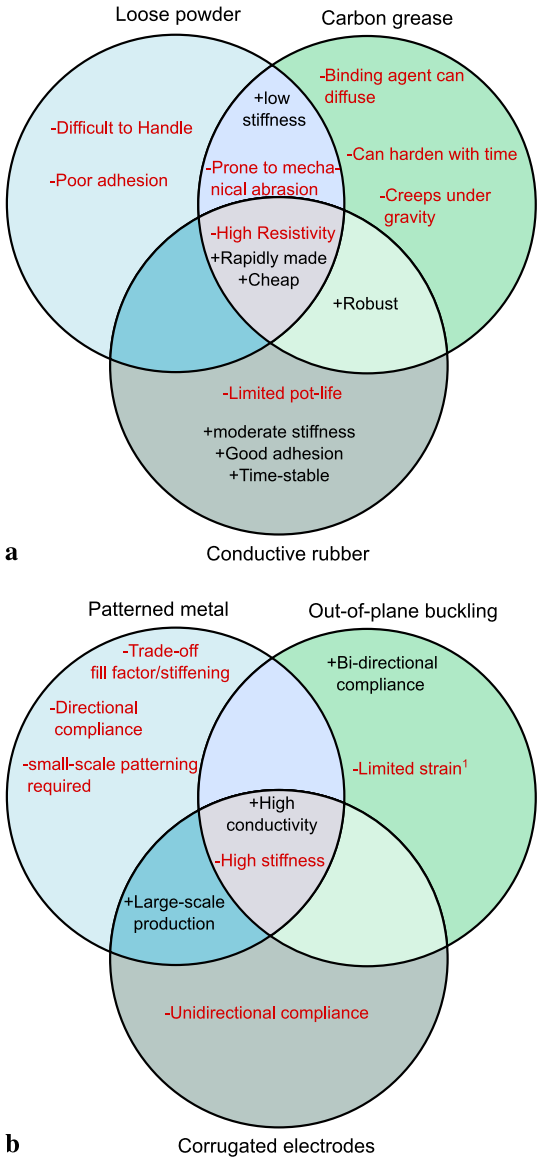

Fig. 21 (**a**) Main characteristics of the carbon-based electrodes presented in Sect. 3. (**b**) Main characteristics of the metallic electrodes presented in Sect. 4. [1]: applies to heat-induced buckling

IC metal thin-film deposition techniques to make compliant electrodes with a low stiffening of the dielectric membrane. These metal electrodes can be patterned using standard microfabrication processes, present a very low surface resistance and good adhesion to the elastomer. They are, however, less compliant than the carbon-based alternatives and may present limitations regarding the direction of actuation. Less conventional techniques are now emerging that combine the advantages of carbon electrodes (high and isotropic compliance) with those of metal electrodes (good conductivity, sub-μm-scale features, excellent adhesion to the substrate, etc.). Several research groups have demonstrated compliant electrodes with advanced features such as intrinsic patternability or presenting a self-healing effect. Different applications require different electrodes: in the lab, carbon electrodes allow fabricating a DEA device in under an hour, but volume manufacturing for consumer goods requires new low-cost, reliable techniques. There is a clear trend towards lower-voltage operation, incorporating self-sensing for a truly *smart* device, as well as an increased interest in miniaturization and integration. For miniaturized applications, it is crucial to minimize the stiffening impact of the electrode on the elastomer. The use of thinner DEAs (which can be stacked to increase the force output) to reduce the actuation voltage is a prerequisite for the widespread adoption of DEAs in everyday applications.

Acknowledgements The authors wish to express their sincere thanks professor Siegfried Bauer for his precious advices regarding the preparation of the manuscript. The authors also thank Samin Akbari, Luc Maffli, and Benjamin O'Brien for their helpful collaboration. This work was supported by the Swiss National Science foundation grant 200020-140394, COST action MP1003, and the Indo Swiss joint research programme (ISJRP).

References

1. R.E. Pelrine, R.D. Kornbluh, J.P. Joseph, Electrostriction of polymer dielectrics with compliant electrodes as a means of actuation. Sens. Actuators A, Phys. **64**(1), 77–85 (1998)
2. F. Carpi, S. Bauer, D. De Rossi, Stretching dielectric elastomer performance. Science **330**(6012), 1759–1761 (2010)
3. C. Keplinger, M. Kaltenbrunner, N. Arnold, S. Bauer, Roentgen's electrode-free elastomer actuators without electromechanical pull-in instability. Proc. Natl. Acad. Sci. USA **107**(10), 4505–4510 (2010)
4. R. Pelrine, R. Kornbluh, Q. Pei, J. Joseph, High-speed electrically actuated elastomers with strain greater than 100 %. Science **287**(5454), 836–839 (2000)
5. F. Carpi, R. Kornbluh, P. Sommer-Larsen, G. Alici, Electroactive polymer actuators as artificial muscles: are they ready for bioinspired applications? Bioinspiration and Biomimetics **6**(4), 045006 (2011)
6. P. Brochu, Q. Pei, Advances in dielectric elastomers for actuators and artificial muscles. Macromol. Rapid Commun. **31**(1), 10–36 (2010)
7. R. Kornbluh, R. Pelrine, J. Eckerle, J. Joseph, Electrostrictive polymer artificial muscle actuators, in *Proceedings of IEEE International Conference on Robotics and Automation*, vol. 3 (1998), pp. 2147–2154
8. R. Kornbluh, R. Pelrine, Q. Pei, S. Oh, J. Joseph, Ultrahigh strain response of field-actuated elastomeric polymers, in *Proceedings of SPIE—The International Society for Optical Engineering*, vol. 3987 (2000), pp. 51–64
9. R. Pelrine, R. Kornbluh, J. Joseph, R. Heydt, Q. Pei, S. Chiba, High-field deformation of elastomeric dielectrics for actuators. Materials Science and Engineering C **11**(2), 89–100 (2000)
10. J.D.W. Madden, N.A. Vandesteeg, P.A. Anquetil, P.G.A. Madden, A. Takshi, R.Z. Pytel, S.R. Lafontaine, P.A. Wieringa, I.W. Hunter, Artificial muscle technology: physical principles and naval prospects. IEEE J. Ocean. Eng. **29**(3), 706–728 (2004)
11. I.A. Anderson, T.A. Gisby, T.G. McKay, B.M. O'Brien, E.P. Calius, Multi-functional dielectric elastomer artificial muscles for soft and smart machines. J. Appl. Phys. **112**(4), 041101 (2012)
12. I.A. Anderson, T. Hale, T. Gisby, T. Inamura, T. McKay, B. O'Brien, S. Walbran, E.P. Calius, A thin membrane artificial muscle rotary motor. Appl. Phys. A, Mater. Sci. Process. **98**(1), 75–83 (2010)
13. S. Wagner, S. Bauer, Materials for stretchable electronics. Mater. Res. Soc. Bull. **37**(3), 207–213 (2012)
14. D.-H. Kim, Y. Lu, N. Huang, J.A. Rogers, Materials for stretchable electronics in bioinspired and biointegrated devices. Mater. Res. Soc. Bull. **37**(3), 226–235 (2012)
15. T. Sekitani, T. Someya, Stretchable organic integrated circuits for large-area electronic skin surfaces. Mater. Res. Soc. Bull. **37**(3), 236–245 (2012)
16. J. Vanfleteren, M. Gonzalez, F. Bossuyt, Y.-Y. Hsu, T. Vervust, I. De Wolf, M. Jablonski, Printed circuit board technology inspired stretchable circuits. Mater. Res. Soc. Bull. **37**(3), 254–260 (2012)
17. D.-H. Kim, N. Lu, R. Ma, Y.-S. Kim, R.-H. Kim, S. Wang, J. Wu, S.M. Won, H. Tao, A. Islam, K. Jun Yu, T.-i. Kim, R. Chowdhury, M. Ying, L. Xu, M. Li, H.-J. Chung, H. Keum, M. McCormick, P. Liu, Y.-W. Zhang, F.G. Omenetto, Y. Huang, T. Coleman, J.A. Rogers, Epidermal electronics. Science **333**(6044), 838–843 (2011)
18. P. Jean, A. Wattez, G. Ardoise, C. Melis, R. Van Kessel, A. Fourmon, E. Barrabino, J. Heemskerk, J.P. Queau, Standing wave tube electro active polymer wave energy converter, in *Proceedings of SPIE—The International Society for Optical Engineering*, vol. 8340, ed. by Y. Bar-Cohen (SPIE, Bellingham, 2012), p. 83400C
19. B.M. O'Brien, E.P. Calius, T. Inamura, S.Q. Xie, I.A. Anderson, Dielectric elastomer switches for smart artificial muscles. Appl. Phys. A, Mater. Sci. Process. **100**(2), 385–389 (2010)
20. F. Carpi, P. Chiarelli, A. Mazzoldi, D. De Rossi, Dielectric elastomer planar actuators for small scale applications, in *Proceedings of SPIE—The International Society for Optical Engineering*, vol. 4763 (2002), pp. 169–172
21. F. Carpi, P. Chiarelli, A. Mazzoldi, D. De Rossi, Electromechanical characterisation of dielectric elastomer planar actuators: comparative evaluation of different electrode materials and different counterloads. Sens. Actuators A, Phys. **107**(1), 85–95 (2003)
22. B. O'Brien, J. Thode, I. Anderson, E. Calius, E. Haemmerle, S. Xie, Integrated extension sensor based on resistance and voltage measurement for a dielectric elastomer, in *Proceedings of SPIE—The International Society for Optical Engineering*, vol. 6524 (SPIE, San Diego, 2007), p. 652415
23. J.C. Huang, Carbon black filled conducting polymers and polymer blends. Adv. Polym. Technol. **21**(4), 299–313 (2002)
24. S.-P. Rwei, F.-H. Ku, K.-C. Cheng, Dispersion of carbon black in a continuous phase: electrical, rheological, and morphological studies. Colloid Polym. Sci. **280**(12), 1110–1115 (2002)

25. L.A. Toth, A.A. Goldenberg, Control system design for a dielectric elastomer actuator: the sensory subsystem, in *Proceedings of SPIE—The International Society for Optical Engineering*, vol. 4695 (2002), pp. 323–334
26. K. Jung, K.J. Kim, H.R. Choi, A self-sensing dielectric elastomer actuator. Sens. Actuators A, Phys. **143**(2), 343–351 (2008)
27. R. Kornbluh, R. Pelrine, J. Joseph, R. Heydt, Q. Pei, S. Chiba, High-field electrostriction of elastomeric polymer dielectrics for actuation, in *Proceedings of SPIE—The International Society for Optical Engineering*, vol. 3669 (1999), pp. 149–161
28. H.F. Schlaak, M. Jungmann, M. Matysek, P. Lotz, Novel multilayer electrostatic solid-state actuators with elastic dielectric, in *Electroactive Polymer Actuators and Devices (EAPAD) 2005*, vol. 5759 (2005), pp. 121–133
29. M. Matysek, P. Lotz, K. Flittner, H.F. Schlaak, High-precision characterization of dielectric elastomer stack actuators and their material parameters. in *Proceedings of SPIE*, vol. 6927 (2008)
30. H. Schlaak, P. Lotz, M. Matysek, *Multilayer Stack Contractile Actuators* (Elsevier, Amsterdam, 2008), pp. 109–122. Chap. 11
31. P. Lotz, H.F. Matysek, M. Schlaak, Fabrication and application of miniaturized dielectric elastomer stack actuators. IEEE/ASME Trans. Mechatron. **16**(1), 58–66 (2011)
32. G. Kofod, Dielectric elastomer actuators. Ph.D. Thesis, The Technical University of Denmark (2001)
33. F. Carpi, C. Salaris, D. De Rossi, Folded dielectric elastomer actuators. Smart Mater. Struct. **16**(2), S300–S305 (2007)
34. M. Aschwanden, D. Niederer, A. Stemmer, Tunable transmission gratings based on dielectric elastomer actuators, in *Electroactive Polymer Actuators and Devices (EAPAD) 2008*, vol. 6927 (SPIE, San Diego, 2008), p. 56
35. P. Lochmatter, G. Kovacs, Design and characterization of an active hinge segment based on soft dielectric eaps. Sens. Actuators A, Phys. **141**(2), 577–587 (2008)
36. G. Kovacs, L. During, Contractive tension force stack actuator based on soft dielectric eap, in *Electroactive Polymer Actuators and Devices (EAPAD) 2009*, vol. 7287, ed. by Y. Bar-Cohen, T. Wallmersperger (SPIE, Bellingham, 2009), p. 72870A
37. F. Carpi, D. De Rossi, Dielectric elastomer cylindrical actuators: electromechanical modelling and experimental evaluation. Materials Science and Engineering C **24**(4), 555–562 (2004)
38. A.P. Gerratt, M. Tellers, S. Bergbreiter, Soft polymer mems, in *Proccedings of IEEE 24th Int Micro Electro Mechanical Systems (MEMS) Conference* (2011), pp. 332–335
39. M. Kujawski, J.D. Pearse, E. Smela, Elastomers filled with exfoliated graphite as compliant electrodes. Carbon **48**(9), 2409–2417 (2010)
40. J.J. Loverich, I. Kanno, H. Kotera, Concepts for a new class of all-polymer micropumps. Lab Chip **6**(9), 1147–1154 (2006)
41. M. Matysek, P. Lotz, T. Winterstein, H.F. Schlaak, Dielectric elastomer actuators for tactile displays, in *Proceedings of 3rd Joint EuroHaptics Conference and Symposium on Haptic Interfaces for Virtual Environment and Teleoperator Systems, World Haptics 2009* (2009), pp. 290–295
42. O.A. Araromi, A.T. Conn, C.S. Ling, J.M. Rossiter, R. Vaidyanathan, S.C. Burgess, Spray deposited multilayered dielectric elastomer actuators. Sens. Actuators A, Phys. **167**(2), 459–467 (2011)
43. M. Aschwanden, A. Stemmer, Low voltage, highly tunable diffraction grating based on dielectric elastomer actuators, in *Electroactive Polymer Actuators and Devices (EAPAD) 2007*, vol. 6524 (SPIE, San Diego, 2007), p. 65241N
44. F.C. Krebs, Fabrication and processing of polymer solar cells: a review of printing and coating techniques. Sol. Energy Mater. Sol. Cells **93**(4), 394–412 (2009)
45. A.P. Robinson, I. Minev, I.M. Graz, S.P. Lacour, Microstructured silicone substrate for printable and stretchable metallic films. Langmuir **27**(8), 4279–4284 (2011)
46. E. Tekin, B.-J. De Gans, U.S. Schubert, Ink-jet printing of polymers—from single dots to thin film libraries. J. Mater. Chem. **14**(17), 2627–2632 (2004)
47. C. Keplinger, T. Li, R. Baumgartner, Z. Suo, S. Bauer, Harnessing snap-through instability in soft dielectrics to achieve giant voltage-triggered deformation. Soft Matter **8**, 285–288 (2012)
48. S. Wang, P. Wang, T. Ding, Resistive viscoelasticity of silicone rubber/carbon black composite. Polym. Compos. **32**(1), 29–35 (2011)
49. S. Rosset, M. Niklaus, P. Dubois, M. Dadras, H.R. Shea, Mechanical properties of electroactive polymer microactuators with ion-implanted electrodes, in *Electroactive Polymer Actuators and Devices (EAPAD) 2007*, vol. 6524 (SPIE, San Diego, 2007), p. 652410
50. A. Pimpin, Y. Suzuki, N. Kasagi, Microelectrostrictive actuator with large out-of-plane deformation for flow-control application. J. Microelectromech. Syst. **16**(3), 753–764 (2007)
51. R. Verplancke, F. Bossuyt, D. Cuypers, J. Vanfleteren, Thin-film stretchable electronics technology based on meandering interconnections: fabrication and mechanical performance. J. Micromech. Microeng. **22**(1), 015002 (2012). doi:10.1088/0960-1317/22/1/015002
52. M. Gonzalez, F. Axisa, M. Vanden Bulcke, D. Brosteaux, B. Vandevelde, J. Vanfleteren, Design of metal interconnects for stretchable electronic circuits. Microelectron. Reliab. **48**(6), 825–832 (2008)
53. A. Pimpin, Y. Suzuki, N. Kasagi, Micro electrostrictive actuator with metal compliant electrodes for flow control applications, in *Proccedings of 17th IEEE International Conference on Micro Electro Mechanical Systems (MEMS)* (2004), pp. 478–481
54. N. Bowden, S. Brittain, A.G. Evans, J.W. Hutchinson, G.M. Whitesides, Spontaneous formation of ordered structures in thin films of metals supported on an elastomeric polymer. Nature **393**(6681), 146–149 (1998). doi:10.1038/30193
55. S.P. Lacour, J. Jones, Z. Suo, S.A. Wagner, S. Wagner, Design and performance of thin metal film interconnects for skin-like electronic circuits. IEEE Electron Device Lett. **25**(4), 179–181 (2004)
56. M. Maghribi, J. Hamilton, D. Polla, K. Rose, T. Wilson, P. Krulevitch, Stretchable micro-electrode array [for retinal prosthesis], in *Conference on Microtechnologies in Medicine Biology 2nd Annual International IEEE-EMB Special Topic* (2002), pp. 80–83
57. A.L. Volynskii, S. Bazhenov, O.V. Lebedeva, N.F. Bakeev, Mechanical buckling instability of thin coatings deposited on soft polymer substrates. J. Mater. Sci. **35**(3), 547–554 (2000)
58. M. Benslimane, P. Gravesen, P. Sommer-Larsen, Mechanical properties of dielectric elastomer actuators with smart metallic compliant electrodes, in *Proceedings of SPIE—The International Society for Optical Engineering*, vol. 4695 (SPIE, Bellingham, 2002), pp. 150–157
59. H.-E. Kiil, M. Benslimane, Scalable industrial manufacturing of deap, in *Proceedings of SPIE*, vol. 7287 (2009)
60. M. Benslimane, H.-E. Kiil, M.J. Tryson, Electromechanical properties of novel large strain polypower film and laminate components for deap actuator and sensor applications, in *Proceedings of SPIE—The International Society for Optical Engineering*, vol. 7642 (2010)
61. K. Sidler, O. Vazquez-Mena, V. Savu, G. Villanueva, M.A.F. van den Boogaart, J. Brugger, Resistivity measurements of gold wires fabricated by stencil lithography on flexible polymer substrates. Microelectron. Eng. **85**(5–6), 1108–1111 (2008). Proceedings of the Micro- and Nano-Engineering 2007 Conference—MNE 2007
62. O. Vazquez-Mena, G. Villanueva, V. Savu, K. Sidler, M.A.F. van den Boogaart, J. Brugger, Metallic nanowires by full

wafer stencil lithography. Nano Lett. **8**(11), 3675–3682 (2008). PMID: 18817451
63. S. Perichon Lacour, S. Wagner, Z. Huang, Z. Suo, Stretchable gold conductors on elastomeric substrates. Appl. Phys. Lett. **82**(15), 2404–2406 (2003)
64. T. Adrega, S.P. Lacour, Stretchable gold conductors embedded in pdms and patterned by photolithography: fabrication and electromechanical characterization. J. Micromech. Microeng. **20**(5), 055025 (2010)
65. L. Guo, S.P. DeWeerth, An effective lift-off method for patterning high-density gold interconnects on an elastomeric substrate. Small **6**(24), 2847–2852 (2010)
66. J.N. Patel, B.L. Gray, B. Kaminska, B.D. Gates, Flexible glucose sensor utilizing multilayer pdms process, in *Proceedings of the 30th Annual International Conference of the IEEE Engineering in Medicine and Biology Society, EMBS'08* (2008), pp. 5749–5752
67. J.N. Patel, B. Kaminska, B.L. Gray, B.D. Gates, A sacrificial su-8 mask for direct metallization on pdms. J. Micromech. Microeng. **19**(11), 115014 (2009)
68. R.M. Diebold, D.R. Clarke, Lithographic patterning on polydimethylsiloxane surfaces using polydimethylglutarimide. Lab Chip **11**, 1694–1697 (2011)
69. I.M. Graz, D.P.J. Cotton, S.P. Lacour, Extended cyclic uniaxial loading of stretchable gold thin-films on elastomeric substrates. Appl. Phys. Lett. **94**(7), 071902 (2009)
70. S. Rosset, M. Niklaus, P. Dubois, H.R. Shea, Metal ion implantation for the fabrication of stretchable electrodes on elastomers. Adv. Funct. Mater. **19**(3), 470–478 (2009)
71. P. Dubois, S. Rosset, S. Koster, J.M. Buforn, J. Stauffer, S. Mikhailov, M. Dadras, N.F. De Rooij, H. Shea, Microactuators based on ion-implanted dielectric electroactive polymer membranes (eap), in *Digest of Technical Papers—International Conference on Solid State Sensors and Actuators and Microsystems, TRANSDUCERS'05*, vol. 2 (2005), pp. 2048–2051
72. P. Dubois, S. Rosset, S. Koster, J. Stauffer, S. Mikhailov, M. Dadras, N.-F. de Rooij, H. Shea, Microactuators based on ion implanted dielectric electroactive polymer (eap) membranes. Sens. Actuators A, Phys. **130**(131), 147–154 (2006)
73. S. Rosset, M. Niklaus, P. Dubois, H.R. Shea, Mechanical characterization of a dielectric elastomer microactuator with ion-implanted electrodes. Sens. Actuators A, Phys. **144**(1), 185–193 (2008)
74. M. Niklaus, H.R. Shea, Electrical conductivity and Young's modulus of flexible nanocomposites made by metal-ion implantation of polydimethylsiloxane: the relationship between nanostructure and macroscopic properties. Acta Mater. **59**(2), 830–840 (2011)
75. G. Corbelli, C. Ghisleri, M. Marelli, P. Milani, L. Ravagnan, Highly deformable nanostructured elastomeric electrodes with improving conductivity upon cyclical stretching. Adv. Mater. **23**(39), 4504–4508 (2011)
76. A. Anders, S. Anders, I.G. Brown, Transport of vacuum arc plasmas through magnetic macroparticle filters. Plasma Sources Sci. Technol. **4**(1), 1–12 (1995)
77. S. Rosset, M. Niklaus, P. Dubois, H.R. Shea, Large-stroke dielectric elastomer actuators with ion-implanted electrodes. J. Microelectromech. Syst. **18**(6), 1300–1308 (2009)
78. K. Wegner, P. Piseri, H. Vahedi Tafreshi, P. Milani, Cluster beam deposition: a tool for nanoscale science and technology. J. Phys. D, Appl. Phys. **39**(22), R439 (2006)
79. S. Akbari, H.R. Shea, An array of 100 μm × 100 μm dielectric elastomer actuators with 80 % strain for tissue engineering applications. Sens. Actuators A, Phys. **186**, 236–241 (2012)
80. M.G. Urdaneta, R. Delille, E. Smela, Stretchable electrodes with high conductivity and photo-patternability. Adv. Mater. **19**(18), 2629–2633 (2007)
81. R. Delille, M. Urdaneta, K. Hsieh, E. Smela, Novel compliant electrodes based on platinum salt reduction, in *Proceedings of SPIE—The International Society for Optical Engineering*, vol. 6168 (2006)
82. R. Delille, M. Urdaneta, K. Hsieh, E. Smela, Compliant electrodes based on platinum salt reduction in a urethane matrix. Smart Mater. Struct. **16**(2), S272 (2007)
83. W. Yuan, T. Lam, J. Biggs, L. Hu, Z. Yu, S. Ha, D. Xi, M.K. Senesky, G. Gruner, Q. Pei, New electrode materials for dielectric elastomer actuators, in *Proceedings of SPIE—The International Society for Optical Engineering*, vol. 6524 (SPIE, San Diego, 2007), p. 65240N
84. W. Yuan, L. Hu, Z. Yu, T. Lam, J. Biggs, S.M. Ha, D. Xi, B. Chen, M.K. Senesky, G. Gruner, Q. Pei, Fault-tolerant dielectric elastomer actuators using single-walled carbon nanotube electrodes. Adv. Mater. **20**(3), 621–625 (2008)
85. G.-K. Lau, S.C.-K. Goh, L.-L. Shiau, Dielectric elastomer unimorph using flexible electrodes of electrolessly deposited (eld) silver. Sens. Actuators A, Phys. **169**(1), 234–241 (2011)
86. S.G. Chun-Kiat, G.-K. Lau, Dielectric elastomeric bimorphs using electrolessly deposited silver electrodes, in *Proceedings of SPIE—The International Society for Optical Engineering*, vol. 7642 (2010)
87. S.H. Low, G.K. Lau, High actuation strain in silicone dielectric elastomer actuators with silver electrodes, in *Proceedings of SPIE—The International Society for Optical Engineering*, vol. 7976 (2011), p. 797636
88. T. Lam, H. Tran, W. Yuan, Z. Yu, S. Ha, R. Kaner, Q. Pei, Polyaniline nanofibers as a novel electrode material for fault-tolerant dielectric elastomer actuators, in *Proceedings of SPIE—The International Society for Optical Engineering*, vol. 6927, ed. by Y. Bar-Cohen (SPIE, Bellingham, 2008), p. 69270O
89. L. Hu, W. Yuan, P. Brochu, G. Gruner, Q. Pei, Highly stretchable, conductive, and transparent nanotube thin films. Appl. Phys. Lett. **94**(16), 161108 (2009)
90. S. Yun, X. Niu, Z. Yu, W. Hu, P. Brochu, Q. Pei, Compliant silver nanowire-polymer composite electrodes for bistable large strain actuation. Adv. Mater. **24**(10), 1321–1327 (2012)
91. S. Shian, R.M. Diebold, A. McNamara, D.R. Clarke, Highly compliant transparent electrodes. Appl. Phys. Lett. **101**(6), 061101 (2012)
92. F. Carpi, G. Frediani, S. Turco, D. De Rossi, Bioinspired tunable lens with muscle-like electroactive elastomers. Adv. Funct. Mater. **21**(21), 4152–4158 (2011)
93. Z. Yu, W. Yuan, P. Brochu, B. Chen, Z. Liu, Q. Pei, Large-strain, rigid-to-rigid deformation of bistable electroactive polymers. Appl. Phys. Lett. **95**(19), 192904 (2009)
94. F. Carpi, G. Frediani, D. De Rossi, Opportunities of hydrostatically coupled dielectric elastomer actuators for haptic interfaces, in *Proceedings of SPIE—The International Society for Optical Engineering*, vol. 7976 (2011)
95. M. Matysek, P. Lotz, K. Flittner, H.F. Schlaak, Vibrotactile display for mobile applications based on dielectric elastomer stack actuators, in *Proceedings of SPIE—The International Society for Optical Engineering*, vol. 7642, ed. by Y. Bar-Cohen (SPIE, Bellingham, 2010), p. 76420D
96. M. Matysek, H. Haus, H. Moessinger, D. Brokken, P. Lotz, H.F. Schlaak, Combined driving and sensing circuitry for dielectric elastomer actuators in mobile applications, in *Proceedings of SPIE—The International Society for Optical Engineering*, vol. 7976, ed. by Y. Bar-Cohen, F. Carpi (SPIE, Bellingham, 2011), p. 797612
97. F. Carpi, D. De Rossi, Improvement of electromechanical actuating performances of a silicone dielectric elastomer by dispersion of titanium dioxide powder. IEEE Trans. Dielectr. Electr. Insul. **12**(4), 835–843 (2005)

98. Z. Zhang, L. Liu, J. Fan, K. Yu, Y. Liu, L. Shi, J. Leng, New silicone dielectric elastomers with a high dielectric constant, in *Proceedings of SPIE—The International Society for Optical Engineering*, vol. 6926 (2008), p. 692610
99. S. Risse, B. Kussmaul, H. Kruger, R. Wache, G. Kofod, Dea material enhancement with dipole grafted pdms networks, in *Proceedings of SPIE—The International Society for Optical Engineering*, vol. 7976 (2011), p. 79760N
100. I.M. Ward, J. Sweeney, *The Mechanical Properties of Solid Polymers* (Wiley, Chichester, 2004)
101. A.P. Gerratt, B. Balakrisnan, I. Penskiy, S. Bergbreiter, Batch fabricated bidirectional dielectric elastomer actuators, in *16th International Solid-State Sensors, Actuators and Microsystems Conference, TRANSDUCERS'11* (2011), pp. 2422–2425
102. A.P. Gerratt, I. Penskiy, S. Bergbreiter, Soi/elastomer process for energy storage and rapid release. J. Micromech. Microeng. **20**(10), 104011 (2010)
103. B. O'Brien, S. Rosset, I. Anderson, H. Shea, Ion implanted dielectric elastomer switches. Appl. Phys. A (2012, accepted). doi:10.1007/s00339-012-7319-2
104. R.D. Kornbluh, R. Pelrine, H. Prahlad, A. Wong-Foy, B. McCoy, S. Kim, J. Eckerle, T. Low, From boots to buoys: promises and challenges of dielectric elastomer energy harvesting. in *Proceedings of SPIE—The International Society for Optical Engineering*, vol. 7976, ed. by Y. Bar-Cohen, F. Carpi (SPIE, Bellingham, 2011), p. 797605
105. S. Chiba, M. Waki, R. Kornbluh, R. Pelrine, Innovative power generators for energy harvesting using electroactive polymer artificial muscles, in *Electroactive Polymer Actuators and Devices (EAPAD) 2008*, vol. 6927, ed. by Y. Bar-Cohen (SPIE, Bellingham, 2008), p. 692715
106. S.J.A. Koh, C. Keplinger, T. Li, S. Bauer, Z. Suo, Dielectric elastomer generators: how much energy can be converted? IEEE/ASME Trans. Mechatron. **16**(1), 33–41 (2011)
107. G. Kang, K.-S. Kim, S. Kim, Note: Analysis of the efficiency of a dielectric elastomer generator for energy harvesting. Rev. Sci. Instrum. **82**(4), 046101 (2011)
108. C.C. Foo, S.J.A. Koh, C. Keplinger, R. Kaltseis, S. Bauer, Z. Suo, Performance of dissipative dielectric elastomer generators. J. Appl. Phys. **111**(9), 094107 (2012)
109. T.G. McKay, B.M. O'Brien, E.P. Calius, I.A. Anderson, Soft generators using dielectric elastomers. Appl. Phys. Lett. **98**(14), 142903 (2011)
110. T. McKay, B. O'Brien, E. Calius, I. Anderson, Self-priming dielectric elastomer generators. Smart Mater. Struct. **19**(5), 055025 (2010)
111. R. Kaltseis, C. Keplinger, R. Baumgartner, M. Kaltenbrunner, T. Li, P. Mächler, R. Schwödiauer, Z. Suo, S. Bauer, Method for measuring energy generation and efficiency of dielectric elastomer generators. Appl. Phys. Lett. **99**(16), 162904 (2011)